05627-20-T

THE UNIVERSITY OF MICHIGAN

COLLEGE OF ENGINEERING
DEPARTMENT OF AEROSPACE ENGINEERING
HIGH ALTITUDE ENGINEERING LABORATORY

Technical Report

Ionospheric Composition Measurements with an R. F. Impedance Probe

E. K. MILLER and H. F. SCHULTE, JR.

Under contract with:

National Aeronautics and Space Administration
Contract No. NASr-54(05)
Washington, D. C.

Administered through:

May 1968

OFFICE OF RESEARCH ADMINISTRATION • ANN ARBOR

THE UNIVERSITY OF MICHIGAN
COLLEGE OF ENGINEERING
Department of Aerospace Engineering
High Altitude Engineering Laboratory

Technical Report

IONOSPHERIC COMPOSITION MEASUREMENTS WITH AN R. F. IMPEDANCE PROBE

E. K. Miller and H. F. Schulte, Jr.

ORA Project 05627

under contract with:

NATIONAL AERONAUTICS AND SPACE ADMINISTRATION
CONTRACT NO. NASr-54(05)
WASHINGTON, D. C.

administered through:
OFFICE OF RESEARCH ADMINISTRATION ANN ARBOR

May 1968

TABLE OF CONTENTS

	Page
List of Figures	iv
Abstract	vi
I. Introduction	1
II. Possible Ion Density Techniques	5
III. Theoretical Development	7
IV. Numerical Examples	15
V. Conclusion	32
References	49

List of Figures

Figure		Page
1.	Impedance of both the cylindrical and spherical antennas as a function of frequency for the sheathless case and for the one and two-ion magnetoplasmas.	35
2.	The two-ion plasma ion-electron hybrid resonance frequency as a function of relative ion abundance with the ion mass ratio a parameter.	36
3.	The two-ion plasma ion-ion hybrid resonance frequency as a function of relative ion abundance with the ion mass ratio a parameter.	36
4.	The two-ion plasma normalized ion-electron hybrid resonance frequency derivative with respect to relative ion abundance with the ion mass ratio a parameter.	37
5.	The two-ion plasma normalized ion-ion hybrid resonance frequency derivative with respect to relative ion abundance with the ion mass ratio a parameter.	37
6.	Spherical probe impedance for the sheathless case in the single ion plasma as a function of frequency with the ion collision frequency a parameter.	38
7.	Spherical probe impedance for the 5 $D\lambda$ ion sheath and electron temperature 1, 500^{O}K in the single ion plasma as a function of frequency with the ion collision frequency a parameter.	39
8.	Impedance of the spherical probe in the two-ion plasma for the sheathless case as a function of frequency with the relative ion abundance ratio a parameter.	40
9.	Impedance of the spherical probe in the two-ion plasma for the 5 $D\lambda$ ion sheath as a function of frequency, with the relative ion abundance ratio a parameter.	41
10.	Spherical probe impedance for the two-ion plasma and the sheathless case as a function of frequency with the heavier ion collision frequency a parameter.	42
11.	Spherical probe impedance for the two-ion plasma and the sheathless case as a function of frequency with the lighter ion collision frequency a parameter.	43
12.	Spherical probe impedance for the two-ion plasma and both the sheathless case and 5 $D\lambda$ ion sheath as a function of frequency.	44

List of Figures (Continued)

Figure		Page
13.	Impedance of the spherical probe for the three-ion plasma and both the sheathless case and 5 D_ℓ ion sheath as a function of frequency.	45
14.	Impedance of the spherical probe for the sheathless case as a function of frequency for a typical ionosphere containing O_2^+, NO^+ and O^+ ions over the altitude range 100 to 300 km.	46
15.	Impedance of the spherical probe for the sheathless case as a function of frequency for a typical ionosphere containing O^+, N^+, He_2^+ and H^+ ions for the altitudes: (a) 600 and 800 km; and (b) 1, 000 and 1, 200 km.	47

Abstract

Consideration is given to extending various methods used for determining electron number density in the ionosphere to ion composition measurements. A technique involving the impedance of an antenna operated in a frequency range on the order of the ion cyclotron frequency to the electron cyclotron frequency appears promising. Theoretical impedance results for some idealized combinations of ions as well as typical ion mixtures encountered in the ionosphere illustrate application of the technique. The advantages and limitations of the impedance probe are discussed.

I. Introduction

Various types of radio frequency (rf) probes have been used for some time now in making measurements of the ionospheric electron number density. Many seemingly different schemes have been developed for this purpose most of which involve the interaction of a single rocket or satellite-borne antenna with the local ionosphere. However, there are only two basically different techniques for which a single antenna is employed; they may be broadly categorized as impedance probes and resonance probes.

In the case of the impedance probe, the first type to be used, the antenna impedance is measured, and by application of some theoretical considerations, the impedance may be used to infer the properties of the medium surrounding the antenna. It is generally desirable to use a single frequency f which is higher than the expected plasma frequencies f_p to be encountered, in which case the impedance of a short antenna is primarily capacitive and is reduced from free space by a factor dependent on the ratio f_p/f. Since the amount of impedance change from the free space value is larger the closer f_p is to f, a number of fixed frequencies may be employed on a rocket experiment where the variation in f_p over the useful part of the flight may be an order of magnitude or more. A disavantage of such impedance measurements is that the antenna impedance may be influenced by factors such as the sheath and non-zero plasma temperature, the earth's magnetic field and vehicle wake effects. These factors are extremely difficult to consider theoretically and thus contribute some error to electron density values obtained from a theoretical approach which ignores them.

The relaxation resonance probe on the other hand does not involve measurements of the antenna impedance. Instead, the antenna is typically excited in a stepped sequence of frequencies (or may also be swept continuously in frequency) with a receiver gated to the transmitting antenna terminals.

A characteristic ringing of the plasma is observed by the receiver as a distinct zero delay echo which persists on the order of milliseconds after the exciting signal is removed, and which occurs most strongly at frequencies which are related to the electron cyclotron, plasma, and upper hybrid frequencies. Since the excitation frequency of the antenna is known and the frequencies of the relaxation resonance do not appear to be significantly affected by the sheath, the electron number density may be determined from the various resonances. This method is thus potentially superior to the impedance probe for measuring the electron number density since frequency can generally be determined more accurately than impedance.

Another type of resonance probe, which we refer to as the Langmuir resonance probe has been used. Its operation depends on the fact that when a superimposed swept frequency rf voltage is applied to a Langmuir probe, an increase in the steady state current to the probe will take place at some characteristic frequency. Since this frequency is not related in a simple way to the electron plasma frequency, being influenced by such factors as the sheath and probe dimensions, the Langmuir resonance probe has some of the same drawbacks as the impedance probe.

We have so far considered plasma probe methods as related to electron density measurements alone. It is reasonable to ask whether the same or similar techniques may be conceivably utilized for determining the concentrations of the various ion species that are present in the plasma. Some consideration has been given to this question by Toepfer and Comisar (1966) who used the Langmuir resonance probe in an effort to measure ion density. Their results were somewhat inconclusive however, since while a resonance of sorts was observed, it was so broad that a density determination from the resonance was consequently quite uncertain. There is in addition a study by Aggson and Kapetankos (1966) which includes the effect of both ions and electrons

on the impedance of a ULF antenna, but which was not intended as a diagnostic tool (more will be said about this later). More recently, Baldeschwieler (1968) has reported on a laboratory experiment for ion mass spectroscopy in which the rf power absorbed by a capacitor between whose plates is interposed the magnetoplasma to be analyzed, is measured as a function of frequency. The absorbed power increases at the cyclotron frequency of the ions in the plasma, so that a knowledge of the magnetic field, which is an experimental parameter, yields the ion mass. This technique is similar in some respects to the method to be discussed here, and to that discussed in a recent article by Blair (1968). Blair does not consider the subject in the detail to be given here, nor does he include a consideration of the sheath problem and the effect of different antenna geometries. The results included herein are felt of sufficient interest in themselves to publish. Both of these works, incidentally, came to the authors' attention after the completion of the investigation described below.

We are interested in seeking other methods for measurement of ion composition because of the difficulties associated with presently available instruments. To date, the Bennett tube RF spectrometer, the conventional magnetic deflcetion spectrometer, the quadrupole spectrometer and even the planar grid retarding potential analyzer have all been used for the measurements of ionospheric composition. In each case, the major problem is laboratory calibration of the instrument. It has not yet been possible to accurately simulate the ionospheric-plasma, vehicle-sheath environment. As a result, the investigator is obliged to determine the instrument mass discrimination characteristics and the approximate sensitivity of his system. To relate the spectrometric results to ambient ion number density, the individual ion responses are summed to obtain a total ion density. If it is assumed that the ion density so derived is

equal to the total electron density, then the specific ion number densities can be determined by this normalization process. If mass discrimination and angle of attack effects occur in the instrument, this must also be properly taken into account.

Since our knowledge of ionospheric physics has now progressed to the point where more accurate and comprehensive measurements are now required it seems desireable to consider methods which might circumvent the calibration and vehicle sheath problems.

It is the purpose of this report to propose a possible method for the measurement of ion composition in the atmosphere which not only avoids the calibration and sheath problems but promises to be less complex and require less power than the spectrometers mentioned above.

II. Possible Ion Density Measurement Techniques

While the ions and electrons both are charged particles in the slightly ionized ionospheric plasma, they are very different in mass so that it does not follow that a method successful for determining the electron number density will necessarily be useful for ion measurements. An example of this is the Langmuir resonance probe just discussed. The fact remains that while the total positive ion number density is equal to the electron number density (assuming no negative or multiply charged ions) the ion plasma frequency is much less than that of the electron plasma frequency. Thus in the region of the ion plasma frequency, the electrons are moving practically in phase with the electric field, thus effectively negating the ion current. This would seem to also rule out the impedance probe for this application, but as will be demonstrated below, the ionospheric magnetic field provides a mechanism for sorting out the ions and electrons in the use of the impedance probe.

The success of the relaxation resonance probe for electron density measurements suggests this as a method deserving perhaps the most serious consideration for ion density measurements. The theoretical approach to the relaxation resonance taken by Dougherty and Monaghan (1966) for the electrons may possibly be extended to consider the ions as well. One might in this way demonstrate the resonances that result when the ions also contribute to the plasma conductivity. Since however, the relaxation type of resonance is apparently dependent on the non-zero plasma temperature for its existence, and because typical satellite and rocket velocities are much greater than the ion thermal velocities, the additional effect of the probe velocity through the plasma would have to be taken into consideration. A physical explanation for the relaxation resonance at the electron plasma frequency as suggested by Fejer and Calvert (1964), is that near f_p the group velocity of the electron acoustical wave, which has a maximum value equal to the electron thermal velocity,

approaches zero and thus nearly matches the slower vehicle velocity so that as a result the receiving antenna remains in a region of strong electric field for a relatively long time. The opportunity then for a similar circumstance to occur involving ion acoustical waves would appear to be small since the ion thermal velocity is almost always much smaller than the vehicle velocity, thus rendering such velocity matching impossible. Thus from a practical viewpoint, and accepting this extremely simplified picture of the relaxation resonance phenomenon, it seems that an ion relaxation resonance experiment does not have great likelihood of success. An additional factor in considering the ion relaxation resonance in a plasma with more than one ion species is the difficulty of sorting out the multiplicity of responses that might be expected, for example at harmonics of the various ion cyclotron frequencies, the various hybrid frequencies etc.

We thus do not consider further in this report the resonance probe technique as a means to measure ion composition and consider an impedance method instead. Since we have found that the impedance probe is subject to some error in the calculation of electron number density due to theoretical difficulty, this does not perhaps appear to be a promising path to pursue. However, it will be subsequently shown that the impedance probe possesses some potentially very attractive properties for ion composition measurements. The next section contains a development of the impedance probe theory, following which some numerical results will be presented.

It should be mentioned that Smith and Brice (1964) have discussed wave propagation in multicomponent (ions and electrons) magnetoplasma, in the course of which they suggested that an active device such as the impedance probe might be useful for ion composition measurements. It was as a result of this reference that the authors became aware of the impedance probe possibilities. To our knowledge however, there are no specific discussions of this problem in the literature, such as follows below.

III. Theoretical Development

A rigorous treatment of a magnetoplasma such as the ionosphere, taking into account ions, electrons and neutrals and utilizing the Boltzmann equation, is extremely complex and generally speaking, impossible to solve without making a number of simplifying assumptions. Even when one reduces the Boltzmann equation to a truncated set of moment equations by performing the appropriate velocity averages, the resulting fluid or hydrodynamic equations are still extremely difficult to solve, particularly when numerical answers are desired. An example of such numerical difficulty is detailed by Chu et. al. (1966) who considered a 3 constituent non-zero temperature ionosphere consisting of positive ions, electrons and neutrals, where it was desired to calculate the propagation constants of the various waves. Because of the birefringence resulting from the ionospheric magnetic field, five modes are possible, two of which are basically electromagnetic in nature and three are acoustical type waves associated with the thermal velocities of the three constituents. The propagation constants are extremely difficult to obtain since they require solving for the complex roots of a complex fifth-order algebraic equation. If in addition, it is desired to find the fields produced by an idealized source in such a medium, such as a point dipole for example, the problem becomes considerably more difficult. Even in the much more simplified case where ion and neutral motion are ignored, the problem requires a great deal of computer time, as shown by Schultz and Graff (1966). The inclusion of particle thermal motion in a treatment of the impedance probe in the two or three constituent plasma is clearly not practical at this time.

There is some evidence provided by a study of the admittance of the infinite cylindrical antenna immersed in a compressible plasma (Miller, 1967a) that the electron thermal motion exerts much less influence over the

antenna admittance when the plasma is anisotropic compared with the isotropic case. There is thus some justification in the present case of the anisotropic ionospheric plasma to neglect the influence of both the electron and ion thermal motion on the antenna impedance. If the plasma is further assumed to be only slightly ionized and a linear theory is used, the neutrals affect the impedance only by means of collision with the ions and electrons. The approach to be used here then is a zero-temperature formulation where the ions and electrons are both considered to have no thermal motion. It will be further assumed that there are no density gradients in the plasma, i.e. the plasma is everywhere uniform, with the proviso that there may exist regions of uniform, but different, density from one another.

The pertinent equations which account for the field variation in the plasma are thus

$$\nabla \times \underline{E} = -i\omega\mu_o \underline{H} \quad , \tag{1}$$

$$\nabla \times \underline{H} = i\omega \epsilon_o \underline{E} - qN\underline{V}_e + qN \sum A_i \underline{V}_i \quad , \tag{2}$$

$$i\omega \underline{V}_e = -\frac{q}{m_e}\underline{E} - \nu_e \underline{V}_e - \frac{q}{m_e}\underline{V}_e \times \underline{B}_o \quad , \tag{3}$$

$$i\omega \underline{V}_i = +\frac{q}{m_i}\underline{E} - \nu_i \underline{V}_i + \frac{q}{m_i}\underline{V}_i \times \underline{B}_o \quad , \tag{4}$$

where $\underline{E}$ and $\underline{H}$ are the time varying electric field and magnetic intensity, ϵ_o and μ_o are the permittivity and permeability of free space, the subscripts e and i denote the electron and i'th ion, $\underline{V}$ is the particle velocity, m the particle mass and N is the electron number density. Further $\underline{B}_o$ is the static magnetic flux density, -q is the electronic charge and A_i the fractional abundance of the i'th ion so that

$$\sum_{i=1}^{I} A_i = 1$$

where there are I different ions. If we take the usual condition of a z-directed field $\underline{B}_o$, then the particle velocities may be obtained as

$$V_{ez} = -\frac{q}{i\omega_e' m_e} E_z \quad , \tag{5a}$$

$$V_{eu} = -\frac{q\omega_{pe}^2}{i\omega_e' m_e N}\left[E_u + \frac{\omega_{he}}{i\omega_e'} E_v\right]\left[1 - (\omega_{he}/\omega_e')^2\right]^{-1} \quad , \tag{5b}$$

$$V_{ev} = -\frac{q\omega_{pe}^2}{i\omega_e' m_e N}\left[E_v - \frac{\omega_{he}}{i\omega_e'} E_u\right]\left[1 - (\omega_{he}/\omega_e')^2\right]^{-1} \quad , \tag{5c}$$

$$V_{iz} = \frac{q}{i\omega_i' m_i} E_z \quad , \tag{6a}$$

$$V_{iu} = \frac{q\omega_{pi}^2}{i\omega_i' m_i A_i N}\left[E_u - \frac{\omega_{hi}}{i\omega_i'} E_v\right]\left[1 - (\omega_{hi}/\omega_i')^2\right]^{-1} \quad , \tag{6b}$$

$$V_{iz} = \frac{q\omega_{pi}^2}{i\omega_i' m_i A_i N}\left[E_v + \frac{\omega_{hi}}{i\omega_i} E_u\right]\left[1 - (\omega_{hi}/\omega_i')^2\right]^{-1} \quad , \tag{6c}$$

and where

$$\omega_{pe}^2 = \frac{q^2 N}{\epsilon_o m_e} \; ; \; \omega_{pi}^2 = \frac{q^2 A_i N}{\epsilon_o m_i} \quad ,$$

$$\omega_{he} = \frac{qB_o}{m_e} \; ; \; \omega_{hi} = \frac{qB_o}{m_i} \quad ,$$

$$\omega_e' = \omega(1+\nu_e/i\omega) \; ; \; \omega_i' = \omega(1+\nu_i/i\omega) \quad .$$

Upon inserting the velocity expressions into (2), we obtain the usual expression

$$\nabla \times \underline{H} = i\omega\epsilon_o \underline{\underline{\epsilon}} \cdot \underline{E} \tag{7}$$

where

$$\underline{\underline{\epsilon}} = \begin{bmatrix} \epsilon_1 & \epsilon' & 0 \\ -\epsilon' & \epsilon_1 & 0 \\ 0 & 0 & \epsilon_3 \end{bmatrix} , \tag{8}$$

and with $$\epsilon_1 = 1 - \frac{X_e U_e}{(U_e^2 - Y_e^2)} - \sum_{i=1}^{I} \frac{X_i U_i}{U_i^2 - Y_i^2} \quad , \tag{9a}$$

$$\epsilon' = \frac{-iX_e Y_e}{U_e^2 - Y_e^2} + i \sum_{i=1}^{I} \frac{X_i Y_i}{U_i^2 - Y_i^2} \quad , \tag{9b}$$

$$\epsilon_3 = 1 - \frac{X_e}{U_e} - \sum_{i=1}^{I} \frac{X_i}{U_i} \quad , \tag{9c}$$

$$X_e = \frac{\omega_{pe}^2}{\omega^2} \; ; \; X_i = \frac{\omega_{pi}^2}{\omega^2} \; ,$$

$$Y_e = \frac{\omega_{he}}{\omega} \; ; \; Y_i = \frac{\omega_{hi}}{\omega} \; ,$$

$$U_e = 1 + \nu_e / i\omega \; ; \; U_i = 1 + \nu_i / i\omega \quad .$$

The problem of deriving a constituitive relation for the magneto-plasma has been straightforward, but the derivation of an impedance expression for a given antenna in such a medium is very difficult. This is a subject which has been pursued quite vigorously in recent years, with many investigators contributing in this area. The various approaches generally differ in the source representation used for a given antenna geometry as well as simplifying theoretical assumptions which may be used. As an example of this Balmain (1964a, 1964b) obtained an analytic expression, using a quasistatic theory, for the impedance of a cylindrical dipole with an assumed triangular current distribution oriented at an arbitrary angle with respect to $\underline{B}_o$. Galejs (1966a, 1966b) has used a variational approach to find the impedance of a finite, insulated cylindrical antenna parallel to $\underline{B}_o$ and a flat strip antenna perpendicular to $\underline{B}_o$. Seshadri (1965a, 1965b, 1966a, 1966b) has also considered various source geometries

in attempting to treat the short cylindrical dipole in an ionospheric-type plasma. Ament et al (1964) and Herman (1964) have also treated this problem. A lengthy list of references has been compiled by Bachynski (1966). It suffices to say that while all those working in this area have as their ultimate goal obtaining the impedance of a real physical antenna in an anisotropic medium, the approaches taken and their proximity to physical reality show a great diversity.

While it has been pointed out that many treatments of the antenna immersed in an anisotropic medium do appear in the literature, very often the results obtained are entirely numerical, or if analytical, would require considerable effort to numerically evaluate. Balmain (1964a, 1964b, 1966) as mentioned above has, however, derived formulas for the impedance of both the spherical and cylindrical antenna in a magnetoplasma which are simple in form and ideal for some numerical calculations. Moreover, a comparison of theoretical values based upon Balmain's formula for the sphere with some experimental ionospheric measurements of the impedance of a 11 cm diameter sphere (Balmain et al 1967) exhibits quite good agreement in the frequency response of the impedance, thus establishing a degree of confidence in the theoretical approach used by Balmain. It does not serve our purpose here to duplicate, even in part, Balmain's development, but instead we simply write down his impedance expressions for both a cylindrical and spherical antenna geometry. Balmain's formula for the cylindrical antenna is given by

$$Z_{in} = \frac{1}{i2\pi\epsilon_o L} \cdot \frac{1}{\epsilon_1 \omega \sqrt{F}} \left[\ln \left[\frac{L}{\rho} \quad \frac{2F}{(a+\sqrt{F})} \right] \quad -1 \right] , \qquad (10)$$

where $2L$ = antenna length ,

ρ = antenna radius ,

$a^2 = \epsilon_1 / \epsilon_3$,

$F = \sin^2 \Theta + a^2 \cos^2 \Theta$,

Θ = angle of antenna axis with respect to magnetic field.

Expression (10) is derived assuming a triangular antenna current distribution and is obtained using a quasistatic theory, i.e., for the limit $\omega\sqrt{\mu_o \epsilon_o} \to 0$. It should be observed that the quasistatic theory is essentially then a low frequency formulation, whose range of validity in relation to the various natural frequencies in the plasma is not entirely clear.

The corresponding expression for a sphere due to Balmain (1966) is given by

$$Z_{in} = \frac{1}{i2\pi \epsilon_o R} \cdot \frac{1}{4\omega \epsilon_1 m} \ln \left(\frac{1+m}{1-m}\right) , \qquad (11)$$

where

R = radius of sphere ,

$m = \sqrt{1 - \epsilon_3 / \epsilon_1} = \sqrt{a^2 - 1} \quad / a$.

This formula is also based on a quasistatic theory and has been developed using different approaches by Pyati (1966) and Meyer (1967).

If it is desired to take into consideration the presence of a positive ion sheath around the antenna, then the spherical geometry is preferable since the sheath may be included more readily there than for the cylindrical case. If in particular, the sheath is a step in electron density from zero to the uniform plasma value of N, at r = S while the ion density is everywhere uniform, then (11) becomes

$$Z_{in} = \frac{1}{j8\omega\pi \epsilon_o} \left\{ \frac{1}{\epsilon_{1s} m_s} \ln \left[\frac{1+m_s}{1-m_s} \right] \left[\frac{1}{R} - \frac{1}{R+S} \right] + \frac{1}{{}_1 m (R+S)} \ln \left(\frac{1+m}{1-m} \right) \right\} \qquad (11a)$$

with the subscript s denoting sheath values, where X_e is zero. Expression (11a) is obtained by adding the sheath impedance and plasma impedance, since they are in series (Balmain, 1966). A more realistic sheath representation could be obtained by allowing for variable electron (and possibly ion) density with radius, a situation that may be readily handled by a series of density steps, so that (11a) would consist of a number of terms similar to the sheath term. This model was used by Balmain et al (1967) in comparing the theoretical and experimental results.

It should be re-emphasized that (10) and (11) are gross approximations to the situation encountered by an actual antenna in the ionosphere, ignoring as they do non-zero temperature effects, antenna motion relative to the medium, sheath asymmetries, plasma non-linearities, and the influence of the rocket or satellite carrier itself on the antenna behavior. In addition, the formulas above are for the steady-state situation, where an implicit assumption is that enough time has elapsed after turning on the antenna excitation at the frequency ω for the transients to die out and the antenna-plasma system to come to equilibrium. When the antenna is swept in frequency, the number of cycles or periods that the excitation frequency is in the vicinity of the various characteristic frequencies of the plasma may be less than required to bring the plasma into equilibrium, while the distance moved by the antenna during one oscillation period is also a factor. These considerations are not of curcial importance at the electron cyclotron frequencies (f_{he}) encountered in the E-region of the ionosphere and above, typically on the order of 1 MHz, since the antenna, even at satellite velocities, moves less than 1 cm during one cyclotron-frequency period, while a frequency sweep rate as high as 1 decade/second means the frequency varies by less than 1 percent from f_{he} for almost 10^4 cycles. When the ions are

considered on the other hand, the cyclotron frequencies in the ionosphere vary from 25 to 800 Hz, so that the corresponding numbers may have extremes of 400 m and 0.2 cycles. This comparison serves to emphasize the differences between the ions and electrons as far as their contribution to the effective plasma permittivity is concerned. For the sake of brevity, the impedance probe technique under discussion will be referred to in the following as the ICIP, standing for "Ion Composition Impedance Probe".

IV. Numerical Examples

It was pointed out above that allowing for the effect of a positive ion sheath around the antenna is more straightforward in the case of the spherical antenna as compared with the cylindrical antenna. Because of this, and also because the spherical antenna impedance has no field-orientation dependence as does that of the cylindrical antenna, thus simplifying the interpretation of the experimental results, most of our subsequent consideration will be devoted to the spherical antenna. In order to demonstrate the similarity of impedance results obtained with the two geometries however, the impedance of both antenna types is shown as a function of frequency in Figure 1 for both a one ion and two ion plasma and the sheathless case with the following parameter values:

$L = 3.048$ m ,

$\rho = 0.01$ m ,

$R = 0.055$ m ,

$f_{pe} = 1$ MHz ,

$f_{he} = 1.47$ MHz ,

$\nu_{ce} = 10^4 \text{sec}^{-1}$,

$\Theta = 0^o$.

One ion plasma -

$A_1 = 1$,

$m_1 = 16$ AMU ,

$\nu_{c1} = 10 \text{ sec}^{-1}$.

Two ion plasma -

$A_1 = A_2 = 0.5$,

$m_1 = 16$,

$m_2 = 1$,

$\nu_{c1} = 10 \text{ sec}^{-1}$,

$\nu_{c2} = 160 \text{ sec}^{-1}$.

The antenna radii and length have been chosen to conform to some experimental parameters while f_{pe}, f_{he} and ν_{ce} are chosen as representative of the ionosphere at a height of 100 to 200 km. The ion masses are appropriate for atomic oxygen and hydrogen, which are the principle ions in the altitude range 500 to 1000 km, this ion combination being selected mainly because of the mass separation, while the ion collision frequencies are selected in the ratio used so that the ion cyclotron minima have similar shapes for the two ions. The question of the impedance dependence on ion mass, relative abundance and collision frequency will be considered separately below.

An examination of the impedance curves for the two antenna geometries shows that while the magnitudes are different, the location in frequency of their respective minima and maxima are the same, for both the one-ion and two-ion plasma. This is a demonstration that the minima and maxima frequencies result from the medium properties and not of the particular antenna geometry, as will be further verified below. The minima in impedance are related to the ion cyclotron frequencies while the maxima are hybrid resonances, the highest one shown involving the ion and electron, and in the case of a multiple-ion plasma, the lower maxima involving the ions only.

Before presenting additional impedance results for the spherical probe, it is worthwhile to investigate the resonance phenomena shown in Fig. 1, to arrive in particular at an understanding of the frequency dependence of the resonance upon ion mass and relative abundance. An examination of (10) and (11) shows that the impedance will become large when $\epsilon_1 \rightarrow 0$, a situation usually referred to as a resonance, and the impedance will become small when ϵ_1 is large, a condition denoted as a cutoff (Allis et al, 1963). If the collision frequencies are all zero, then ϵ_1 can become exactly zero, so that impedance infinities would thus occur when

$$1 - \frac{X_e}{1-Y_e^2} - \sum_{i=1}^{I} \frac{X_i}{1-Y_i^2} = 0 \quad . \tag{12a}$$

Impedance zeros would result when

$$\frac{1}{1 - \frac{X_e}{1-Y_e^2} - \sum_{i=1}^{I} \frac{X_i}{1-Y_i^2}} = 0 \quad . \tag{12b}$$

It is easy to see that impedance zeroes occur whenever

$$Y_e = 1 \quad \text{or} \quad Y_i = 1 \ , \tag{13}$$

i.e., at the various ion and electron cyclotron frequencies. If the collision frequencies are non-zero, impedance minima occur at frequencies where ϵ_1 has maxima, and for small ν/ω values, these impedance minima are not appreciably shifted from the Y_e or $Y_i = 1$ values. The effect of a variable collision frequency will be considered further in the following; for the moment we assume zero collision frequencies. It should be noted that impedance zeroes or infinities are of course not physically possible, the non-linear plasma behavior limiting the field magnitudes in the cutoff and resonance regions.

The cutoff frequencies, or the impedance zeroes (or minima), are thus seen to be determined by the respective cyclotron frequencies of the various ions and the electrons as shown by Fig. 1. Since the cyclotron frequency is mass dependent only and not a function of the particle number density, we see that the cyclotron cutoff frequencies serve to identify the masses of the constituent plasma ions. The resonance frequencies, which are solutions to (12a), are not so simply stated, and since they may involve more than one plasma constituent or characteristic frequency, are denoted as hybrid resonances. An exact solution for these hybrid frequencies, when several ions are present, is very complex analytically. If we consider only a two-ion plasma, and make some reasonable approximations, (these resonance and cutoff frequencies have been discussed by Smith and Brice, 1964) the hybrid resonance frequencies may be easily obtained however.

The highest hybrid resonance occurs in the vicinity of the electron plasma and cyclotron frequencies. Since, in this area, $X_i << X_e$ and $Y_i << 1$, then approximately from (12a),

$$Y_e^2 + X_e = 1 \ ,$$

or

$$f_t^2 = f_{he}^2 + f_{pe}^2 \ . \tag{14a}$$

The frequency f_t is most often called the upper hybrid frequency. Another hybrid resonance can occur between the ion plasma frequencies and electron plasma frequency, and in this range $Y_i << 1$ still holds while in addition $Y_e^2 >> 1$.

Thus $$\sum_{i=1}^{I} X_i \simeq 1 + \frac{X_e}{Y_e^2} \ .$$

If we denote the ion to electron mass ratio by M_i, then

$$X_i = X_e A_i / M_i \ .$$

Thus we have

$$f_{ie}^2 = \frac{f_{pe}^2 \, f_{he}^2}{f_t^2} \sum \frac{A_i}{M_i} \tag{14b}$$

for the ion-electron hybrid resonance frequency, f_{ie}. The lowest hybrid resonance occurs in the vicinity of the ion cyclotron frequencies, and if we rewrite (12a) in the form

$$1 - \frac{X_e}{1 - Y_e^2} - X_e \sum_{i=1}^{I} \frac{A_i M_i}{M_i^2 - Y_e^2} = 0 \ ,$$

we see that since $Y_e^2 \sim M_i^2$ then the ion terms predominate in this expression, so that for two ions we have for the ion-ion hybrid resonance,

$$f_j^2 = \frac{f_{he}^2}{M_1 M_2} \left[\frac{A_1 M_1 + A_2 M_2}{A_1 M_2 + A_2 M_1} \right] \ . \tag{14c}$$

The subscript j will be used to number the ion-ion resonances, in order of increasing magnitude there being I-1 resonances for the I-ion plasma. Since I = 2 in this example, j = 1 only.

An examination of the resonance frequencies (14) and the cutoff frequencies (13) reveals that a cutoff occurs between each resonance, i.e., the impedance maxima are separated by impedance minima. The minima identify the masses of the various plasma constituents, while the maxima contain information about the relative abundances. For example, having determined M_1 and M_2 from (13), (14c) may be used to find the ratio of A_1 to A_2, f_{he} being obtained from a knowledge of the earth's magnetic field. Application of (14b) then leads to a relationship between f_{pe} and A_1 for example, so that a separate measurement of f_{pe} (possible from a relaxation resonance) will then determine A_1. While f_{pe} must be known for an absolute determination of ion number density, the relative abundances may be found from ion hybrid resonances and using

$$\sum_{i=1}^{I} A_i = 1 \quad . \tag{15}$$

Consequently, (14b) could then be used to find f_{pe} from the known A_i and M_i, so that another method is thus available for finding the electron number density. Since the ion-electron hybrid resonance frequency is sheath dependent whereas the ion-ion hybrid resonances are not, a comparison between f_{pe} obtained from (14b) with a relaxation resonance measurement may provide information of value about the sheath thickness and consequently, the electron temperature.

While the discussion above has been confined to the two ion plasma, the same principles apply to the I-ion plasma. The I-1 ion-ion hybrid resonance frequencies, together with (15) provide necessary information for converting the I relative ion abundances into absolute concentrations. The most attractive feature of using this impedance probe technique for measuring the ion concentrations is that it is the frequencies at which the various resonances and cutoffs occur, which are properties of the medium, rather than the absolute antenna

impedance, which supply the composition information. The measurement is thus potentially less subject to error and theoretical misinterpretation since the frequency can be generally measured more accurately than the impedance, while in addition the cutoff and resonance frequencies may more reasonably be expected to be correctly predicted by the theory than the absolute antenna impedance.

It is natural to ask at this point what sort of accuracy is required in the frequency measurement to obtain a desired accuracy in the relative ion abundances. In addition, it is pertinent to inquire about the sensitivity of the various resonance frequencies to changing relative ion abundances, since (14b) and (14c) both contain a dependance on the ion mass and concentration. Consequently, we present in Figs. 2 and 3 respectively the ion-electron hybrid resonance frequency, f_{ie} and the ion-ion resonance frequency $f_{j=1}$ as a function of relative ion abundance A_1 ($A_2=1-A_1$) for $f_{pe}=1.47$ MHz and $f_{he}=1.47$ MHz and various ion mass ratios, with the mass M_1 being 32 AMU, corresponding to molecular oxygen. We see that the ion-electron hybrid resonance is on the order of 10 KHz, or about $10^{-2}f_{pe}$, while the ion-ion hybrid resonance is on the order of 100 Hz. It should be again noted that the ion-ion hybrid resonance is not dependent on f_{pe}, but only on the relative ion abundances and masses.

The sensitivity of the resonances to changing A_1 is seen to be very dependent on the ratio M_1/M_2, and for $M_1/M_2 \leq 2$($M_1/M_2 = 32/30$ corresponds to O_2^+ and NO^+), a very large change in relative abundance produces a very small change in the resonance frequency. This is shown more forcefully in Figs. 4 and 5 where the magnitudes of the derivatives of the resonance frequencies with respect to A_1 divided by the resonance frequency are shown as a function of A_1. The fractional change in the resonance frequency caused by a specified change in A_1 is obtained then by multiplying the ordinate value by the change in A_1. We see then, as an example, that at $A_1=0.5$, a change in A_1 of ΔA_1 produces a

fractional change in the ion-ion hybrid resonance of from $6\times10^{-2}\triangle A_1$ for $M_1/M_2=1.07$ to $1.9\triangle A_1$ for $M_1/M_2=32$. Corresponding values for the ion-electron hybrid resonance are $3\times10^{-2}\triangle A_1$ and $8.8\times10^{-1}\triangle A_1$ respectively. If frequency changes of 0.05 are accurately detectable, then relative abundance changes will be measureable only for M_1/M_2 ratios on the order of 2 or larger, where fractional changes in A_1 on the order of 0.1 or less may be seen from the ion-ion resonance. It should again be noted that the ion-electron hybrid resonance frequency is not required to obtain the relative ion abundances, but is useful in establishing their absolute concentrations, and since its location is proportional to the electron density, its relative insensitivity to changing ion composition is not too important.

It is relevant to mention here that our discussion of the impedance probe has thus far been confined to the impedance magnitude, rather than considering for example, the resistive and reactive impedance components separately, i.e., the impedance phase. Since the antenna reactance changes sign as the frequency passes through each resonance or cutoff for small collision frequencies, the antenna reactance would alone be sufficient to determine these frequencies. However, the impedance magnitude is more readily measured than the separate components, so that from an experimental standpoint, it may be preferrable to deal with the impedance magnitude. None the less, this certainly does not rule out the desirability of attempting to measure the impedance phase, as well as its magnitude, since the additional information resulting from this may prove very fruitful. For example, the reactance zero shifts away from the resonance and cutoff frequencies, for sufficiently large collision frequencies, so that the possibility exists of using this property to also obtain the corresponding collision frequencies. In this preliminary study however, we will confine the results to the impedance magnitude alone.

With these preliminary considerations behind us, it is now worthwhile to present some impedance curves which illustrate the role of the other parameters, such as collision frequency and the sheath thickness, as well as to show graphically the impedance behavior with changing ion abundance. Figure 6 shows the impedance of the 11 cm diameter spherical antenna and a single ion plasma (M_1 = 16 AMU) for the sheathless case as a function of frequency, with the ion collision frequency a parameter. We see that the cyclotron cutoff at 50 Hz is more sensitive to the changing collision frequency than the ion-electron resonance at about 5 KHz, and as might be expected, as the collision frequency increases, the impedance minimum is broadened and made shallower, until it finally disappears altogether. It appears that when ν/ω becomes very much larger than unity, the minimum at the cyclotron cutoff is washed out, a phenomena also to be expected at the ion-electron resonance, were ν_1 made large enough, in this case on the order of 10^5sec^{-1}. The curves in Fig. 6 demonstrate very graphically the limitation of the ICIP method established by ion collisions. A similar behavior could be expected at the ion-electron resonance when the electron collision frequency becomes large enough. Ion and electron collisions with neutral particles thus serve to establish a lower altitude limit in the ionosphere to the ICIP usefulness. While the impedance magnitude rather than the cutoff and resonance frequencies may conceivably be used to extend the useful operating range to lower altitudes, the major advantage of the ICIP technique as a frequency sensitive measurement are then lost, so this does not appear to be a promising course to consider.

The spherical antenna impedance is shown for the 5 Debye length (D_ℓ) ion sheath in Fig. 7 for the same antenna diameter and plasma parameters as used in Fig. 6, where

$$D_\ell = \sqrt{(kT_e \epsilon_o / N)} \Big/ q,$$

$$S = R + 5 D_\ell ,$$

where k is Boltzmann's constant and an electron temperature T_e of 1, 500°K has been used in the calculations. There are two significant differences between the results of Figs. 6 and 7. Firstly, the impedance magnitude for the $5D\ell$ ion sheath is 1 to 2 orders of magnitude greater than for the sheathless case. Secondly, the ion-electron resonance frequency has been shifted upward, from about 4.9 KHz for the sheathless case to about 5.8 KHz for the $5D\ell$ sheath. Since the frequency of the ion-electron resonance for the sheathless case may be verified to satisfy (14b), the shift in the predicted value from (14b) may be taken to indicate the presence of a sheath. If the electron temperature is available from a separate measurement, and the ion sheath thickness is known, then the electron temperature emerges instead as a determinable quantity. It is important to note that the only resonance frequency which is sensitive to this sheath model is the ion-electron resonance, as will be subsequently demonstrated.

The results above which show the effect of a variable ion collision frequency or the presence of an ion sheath have been for the one-ion plasma. The next series of graphs will exhibit the impedance variation for a two-ion plasma. In Fig. 8 is shown the spherical antenna impedance as a function of exciting frequency for the sheathless case, with the relative abundance of the two ions of 16 and 1 AMU (corresponding to O^+ and H^+ ions) a parameter. The impedance curves on this graph show rather strikingly the shifting in location of the ion-ion resonance and ion-electron resonance with changing ion abundance. It is especially interesting to see that the depth of the impedance minimum at the ion cyclotron cutoff decreases with decreasing density of the particular ion. The dependence of the resonance frequencies upon the ion mass ratios and abundance is seen to agree with that predicted by (14b) and (14c), where an increased proportion of the heavier ion is shown to shift the ion-electron

resonance downward in frequency, while the ion-ion resonance is shifted upward. The ion-ion resonance of course disappears when only one ion is present, as shown by Fig. 8.

Some curves corresponding to those of Fig. 8 are shown in Fig. 9 for the case of a 5 D_ℓ thick ion sheath. As for the one-ion plasma, the impedance is increased one to two orders of magnitude compared with the sheathless case, and again the ion-electron resonance frequency is shifted upward compared with the sheathless case. The ion-ion resonances occur at the same frequencies for both the sheathed and sheathless cases, however, as do the ion cutoff frequencies.

In Figs. 10 and 11 are shown the probe impedance for the two ion plasma, again for the sheathless case, with ν_1 a parameter in Fig. 10 and ν_2 a parameter in Fig. 11. It may be observed that only the cyclotron cutoff of the ion whose collision frequency is increasing is appreciably affected. The ion-electron resonance is decreased in magnitude as the ion collision frequency is increased, and may even be shifted in frequency when ν_2 is made large enough. In addition the ion-ion resonance is seen to be eliminated at the higher ion collision frequency values. Figure 12 shows the impedance for both the sheathless and 5 D_ℓ thick ion sheath when the ion collision frequencies are both large, with $\nu_1 = 10^4 \text{sec}^{-1}$ and $\nu_2 = 1.6 \times 10^5 \text{sec}^{-1}$. A very broad impedance maximum is seen to occur in the vicinity of the ion-electron resonance shown in the previous graphs, but it seems clear that when the ion collision frequencies are sufficiently large, little useful information may be expected to be obtained from the impedance probe. Incidentally, the combination of collision frequencies and ion masses used in this sequence of graphs are not realistic in terms of the actual ionosphere, but have been used to illustrate the influence of these factors on the antenna impedance.

In order to further illustrate the impedance probe characteristics in a more complex plasma environment, Fig. 13 presents the impedance as a function of frequency for a three ion plasma with M_1, M_2 and M_3 equal to 16, 4 and 1 AMU (corresponding to O^+, He_2^+ and H^+), and $A_1=A_2=A_3=1/3$. The ion collision frequencies are ν_1= 10, ν_2=40 and ν_3=160 sec^{-1}, chosen as before in ratios such that the cyclotron cutoffs would have similar shapes. Results are shown in Fig. 13 for both the sheathless case and a $5D_\ell$ thick ion sheath. It may be seen that except in the area of the ion-electron resonance the impedance for the sheathless case is about one order of magnitude less than that for the $5D_\ell$ sheath; at the ion-electron resonance the difference is more than two orders of magnitude. There is also an upward shift in the ion-electron resonance frequency due to the sheath, but the cyclotron cutoffs and ion-ion resonances are not shifted by the sheath, a result found previously for the two-ion plasma.

The curves of Fig. 13 are quite striking and appear to indicate that the ICIP may be promising for ionospheric diagnostics. It must be emphasized however, that the plasma parameters used for Fig. 13 are idealized as far as the ion mass ratios and collision frequencies of the real ionosphere are concerned. It should be remembered for example, from the graphs of Figs. 2 and 3 that the closer the ion masses, the less sensitive is the ion-ion resonance to changing relative ion abundance. Thus in order to demonstrate the results which may be more typical of the actual ionosphere, we present in Figs. 14 and 15 the antenna impedance vs. frequency curves calculated from some actual measured ion composition profiles in the ionosphere.

The results of Fig. 14 are shown over the altitude range 100-300 km at 50 km intervals using the ion composition measurements of Johnson, Meadows and Holmes (1958) taken from a rocket shot on 20 November, 1956, together with

ion and electron collision frequencies and electron densities for a "hot" ionosphere given by Chapman (1956). The numerical values used for these parameters are shown on the graph. The curve for 100 km altitude is seen to be very flat, and except for frequencies greater than about 100 KHz, almost independent of frequency. This impedance behavior is caused by the relatively large collision frequencies for this height in the ionosphere, which as may be deduced from the impedance formula given by (11), has the effect of cancelling the $1/\omega$ term in the impedance over a relatively large frequency range.

At an altitude of 150 km, the collision frequencies are considerably smaller than at 100 km and the impedance begins to show the frequency dependence previously found for the more idealized plasma models. It should be emphasized however, that there are three ions present in the plasma, but because of the still comparitively high collision frequency, only one broad minimum is seen in the impedance. Proceeding upward another 50 km to 200 km, we see that two minima now occur, one at about 50 Hz, corresponding to O^+, and the other at about 26 Hz, which appears to be the result of the separate minima for NO^+ and O_2^+ coalescing due to the still appreciable collision frequencies and the closeness of their respective masses. Finally at 250 km altitude, three impedance minima are seen corresponding to the three ions present in the model ionosphere which has been used. Since the NO^+ and O_2^+ ions are now present with an abundance for each of about 7 percent of the total ion population, their cyclotron cutoffs and the ion-ion resonance between are not very pronounced. The 300 km curve is for a one-ion plasma, consisting of O^+ alone, and has then one minimum at the O^+ cyclotron frequency. In each of the curves from 150 km and up, there is seen to be an upward shift in the ion-electron resonance, which is caused mainly by the increasing electron density with altitude. For two of the curves however, at 150 and 200 km, the electron density is the same, the upward

shift here resulting from the increased relative abundance of the lighter mass ion.

As the last graph of this series, Fig. 15 shows the probe impedance vs. frequency curves for an altitude range of 600 to 1200 km at 200 km intervals. The ion and electron density values are taken from the results summarized by Ghosh (1967). Since the ion and electron collision frequencies are negligible in this altitude range, they have been set equal to zero for purposes of the calculations. The four curves are shown on two separate graphs for the sake of clarity, since due to the use of zero collision frequency values the minima and maxima are quite sharp and may overlap. Incidentally, a constant value for f_{he} of 1.47 MHz has been used for these calculations so that the shifts in the ion-ion resonance would be due to changes in fractional abundances only. In reality, the magnetic field would decrease significantly in the altitude range considered here. The change of magnetic field with increasing altitude could easily be taken in account in the reduction of experimental data.

The curves of Fig. 15 show that cyclotron cutoffs occur for each ion in spite of the fact that the fractional abundance of a particular ion may be as low as 1 percent. It thus appears that identification of the less abundant ions present in the ionosphere would be feasible, although their relative concentrations may be difficult to obtain accurately because of the small shifts in the various ion-ion resonances which result from fairly substantial changes in the relative abundances. The ion-ion resonances are seen to shift more when located between the cyclotron cutoffs of ions whose masses differ by the larger amounts, a feature mentioned in the previous discussion.

It is worthwhile to mention at this point that our discussion of the antenna impedance has neglected the possibility of the probe interacting with the plasma in ways other than the exciting of an electromagnetic field which is modified by the effective permittivity of the surrounding plasma. In a somewhat related

study, Aggson and Kapetankos (1966) considered the source impedance of an antenna in the ionosphere which interacts with the plasma by drawing both an ion and electron current, as well as a photo-emission current, supplying the resulting current to a connected receiver.

Their numerical results for a cylindrical antenna 100 cm in length and 1 cm in diameter moving with satellite velocity indicate that the impedance is primarily resistive for frequencies below 100 KHz and altitudes of 200 to 1000 km in the daytime, the nighttime resistive domain occuring for somewhat lower frequencies. Above these frequencies the impedance becomes primarily capacitive. Over the 200 to 1000 km altitude range, the antenna impedance may vary by more than an order of magnitude, being as low as 10^4 ohms in the daytime, with the nighttime value roughly an order of magnitude larger. Because the minimum impedance value obtained by Aggson and Kapetankos is on the order of the largest impedance values found in Figs. 14 and 15 where the appropriate ionospheric parameter values have been used, it appears that the influence of charge collection from the plasma by the antenna on the impedance would be small, since the two impedances would be in parallel. This comparison is not wholly valid because Aggson and Kapetankos used a cylindrical geometry in their calculations, while we have used a spherical geometry. In any case, the effect of charge collection and photo-emission by the antenna may be largely minimized by coating the antenna with a suitable dielectric material.

Also an important consideration here is the applicability of the sheath description used for these calculations. We have already noted the increased impedance which results when the antenna is surrounded by an ion sheath a few electron Debye lengths thick, because of the decreased sheath conductivity when ions only are present in the sheath. If the ions too do not contribute to the sheath conductivity, perhaps due to the motion of the antenna

through the plasma so that the ions move through the sheath without appreciably interacting with the rf fields there, then as shown by the first term of (11a) with $\epsilon_{1s} \sim 1$, $Z_{in} \sim 10^8$ Ohms at f = 10^2 Hz. This large value of impedance would effectively screen the probe from the effect of the plasma, contained in the second term of (11a), so that the frequency dependence of the probe would be f^{-1} over the frequency range of interest here. A behavior of this sort is reported in a recent experiment conducted by Shawhan and Gurnett (1967). This possibility suggests that it may be desirable to decrease the free-space probe impedance to reduce the series sheath component, or an attractive alternative may be a passive, noise-monitoring probe to look for noise enhancement at the various characteristic frequencies, an approach suggested by Smith and Brice (1964).

Out attention has thusfar been principally directed towards demonstrating some of the characteristics of the ICIP, and we have dealt only briefly with the problem of working backward from the measured impedance curves to the ion abundances. Since this would of course be the ultimate goal of using the technique, it is certainly worthwhile here to give some consideration to this question. The accomplishment of this task requires that having identified the I ion masses from the cyclotron cutoffs and having obtained the I-1 ion-ion resonance frequencies, we use (12a) together with (15) to solve for the I A_i.

A drawback of (12a) as it stands is that the electron plasma frequency appears in it and in order to obtain f_{pe}, the ion-electron resonance frequency must also be utilized. This is not too desirable since it has been shown that the ion-electron resonance may be shifted by the presence of a sheath. If (12a) is rewritten it can be shown however, that only the last term contributes significantly at the ion-ion resonances. We write (12a) in the form

$$1 - \frac{f_{pe}^2}{f_j^2 - f_{he}^2} - f_{pe}^2 \sum_{i=1}^{I} \frac{A_i M_i}{f_j^2 M_i^2 - f_{he}^2} = 0 \qquad (12a)'$$

where f_j is the j'th ion-ion resonance frequency. Since the f_j frequencies lie between the ion-cyclotron frequencies, which are given by f_{he}/M_i, then the second term above is approximately

$$- \frac{f_{pe}^2}{f_j^2 - f_{he}^2} \approx \frac{f_{pe}^2}{f_{he}^2} \quad .$$

Since the separate parts of the denominator of the third term are $\sim f_{he}^2$, then it is approximately

$$\left| - f_{pe}^2 \sum_{i=1}^{I} \frac{A_i M_i}{f_j^2 M_i^2 - f_{he}^2} \right| \sim \frac{f_{pe}^2}{f_{he}^2} \sum_{i=1}^{I} A_i M_i >> \frac{f_{pe}^2}{f_{he}^2} \quad .$$

Thus the third term is on the order of M_i larger than the second term. Similarly, since $f_{pe}/f_{he} \sim 1$ for most of the ionosphere of interest to us, the third term is on the order of M_i larger than the value of unity of term one.

Thus $(12a)'$ is given very accurately at the ion-ion resonances by

$$\sum_{i=1}^{I} \frac{A_i M_i}{f_j^2 M_i^2 - f_{he}^2} = 0 \; ; \quad j = 1, 2, \ldots\ldots, I-1 , \qquad (16)$$

which together with

$$\sum_{i=1}^{I} A_i = 1$$

forms a system of I equations in the I unknown A_i. It is implicitly assumed here that f_{he} is known, while the M_i are determined from the impedance minima.

As an example, the f_j from the sheathless curve of Fig. 13 and the 250 km curve of Fig. 14 have been used to calculate the A_i which can then be compared with the actual A_i values used to obtain the curves. The results obtained are shown in Table I. Also shown are the values obtained for f_{pe}, which come from

$$f_{pe}^2 = \frac{f_{ie}^2 f_{he}^2}{(f_{he}^2 \sum_{i=1}^{I} A_i/M_i - f_{ie}^2)} \tag{17}$$

It is immediately evident that the results from Fig. 13 where the ion masses are more separated and of equal abundance are more accurate than the situation for Fig. 14 where the ion mass separations are not so large and the abundances are at a great disparity. The calculated abundances from the curves of Fig. 13 vary from the actual values by at most 3.5%, and the calculated electron plasma frequency is within 2.3% of that used. The calculated results of Fig. 14 are at variance from the actual values by as much as 36% for the ion abundance and 10% for the electron plasma frequency. It is noteworthy however, that the most abundant ion of Fig. 14 is calculated to an accuracy within 1% of the actual value. These results are encouraging and hardly surprising, since we might expect that the less the ion abundance the less the absolute accuracy which may be obtained particularly when the masses are at the same time close together. In addition, it is apparent from (17) that f_{pe} is quite sensitive to error in the value of f_{ie}, so that the difference between the calculated and acutal values for f_{pe} shown in Table I may be largely due to this source. Since the sum $\sum A_i/M_i$ also plays a role in determining f_{pe}, errors in A_i may be also reflected in an incorrect f_{pe} value.

V. Conclusion

This investigation has considered the possibility of measuring ion composition in an ionospheric-type plasma by methods other than the spectrometric techniques currently in use. A motivation for this work has been the desire to obtain an ion composition measurement scheme that may be inherently much less complex and less prone to calibration error than are current spectrometers designed for use in the ionsophere.

A consideration of various techniques that are used for electron number density measurements and the feasibility of extending them to ion composition determination has led to the impedance probe as potentially the most promising method to pursue. Based on the quasistatic formulation of Balmain for the zero-temperature magnetoplasma, the ICIP is found to exhibit minima and maxima in impedance as a function of frequency. The impedance minima supply information about the relative masses of the various constituent ions, reducing to absolute ion masses if the ionospheric magnetic field is known. From the impedance maxima is obtained the relative fractional abundances of the various ions, as well as potential information concerning the electron density, electron temperature and sheath thickness.

The most attractive feature of the ICIP is that it is the frequencies at which the impedance minima and maxima occur, rather than the absolute impedance magnitude, which supplies the ion composition. A frequency measurement is generally more easily performed to a given accuracy than an impedance measurement, while in addition, the various characteristic frequencies are dependent on the plasma medium and likely to be less subject to theoretical uncertainties than is the absolute antenna impedance.

The theoretical approach used is certainly limited in sophistication, neglecting as it does, non-zero temperature effects, probe velocity through the medium, and possible non-linear plasma behavior. Consequently, the results obtained in this study, while intriguing and quite promising, cannot be accepted without some caution. It appears that further theoretical effort to bring the actual physics and assumed model closer together is desireable, particularly to determine the limitations of a steady-state analysis in relation to the actual dynamic problem of an antenna moving through a non-zero temperature ionosphere. Some experimental results could be very informative in demonstrating the feasibility of the technique and determining the desirability of further theoretical effort.

Table I

Fig. 13; f_1 = 94 Hz; f_2 = 430 Hz; f_{ie} = 13 KHz

	M_i	M_2	M_3	A_1	A_2	A_3	f_{pe}
Actual	16	4	1	0.333	0.333	0.333	1 MHz
Calculated				0.325	0.345	0.330	1.023 MHz

Fig. 14; f_1 = 26 Hz; f_2 = 28.5 Hz; f_{ie} = 7.8 KHz

Actual	24	30	16	0.069	0.069	0.862	4.50 MHz
Calculated				0.088	0.044	0.868	4.05 MHz

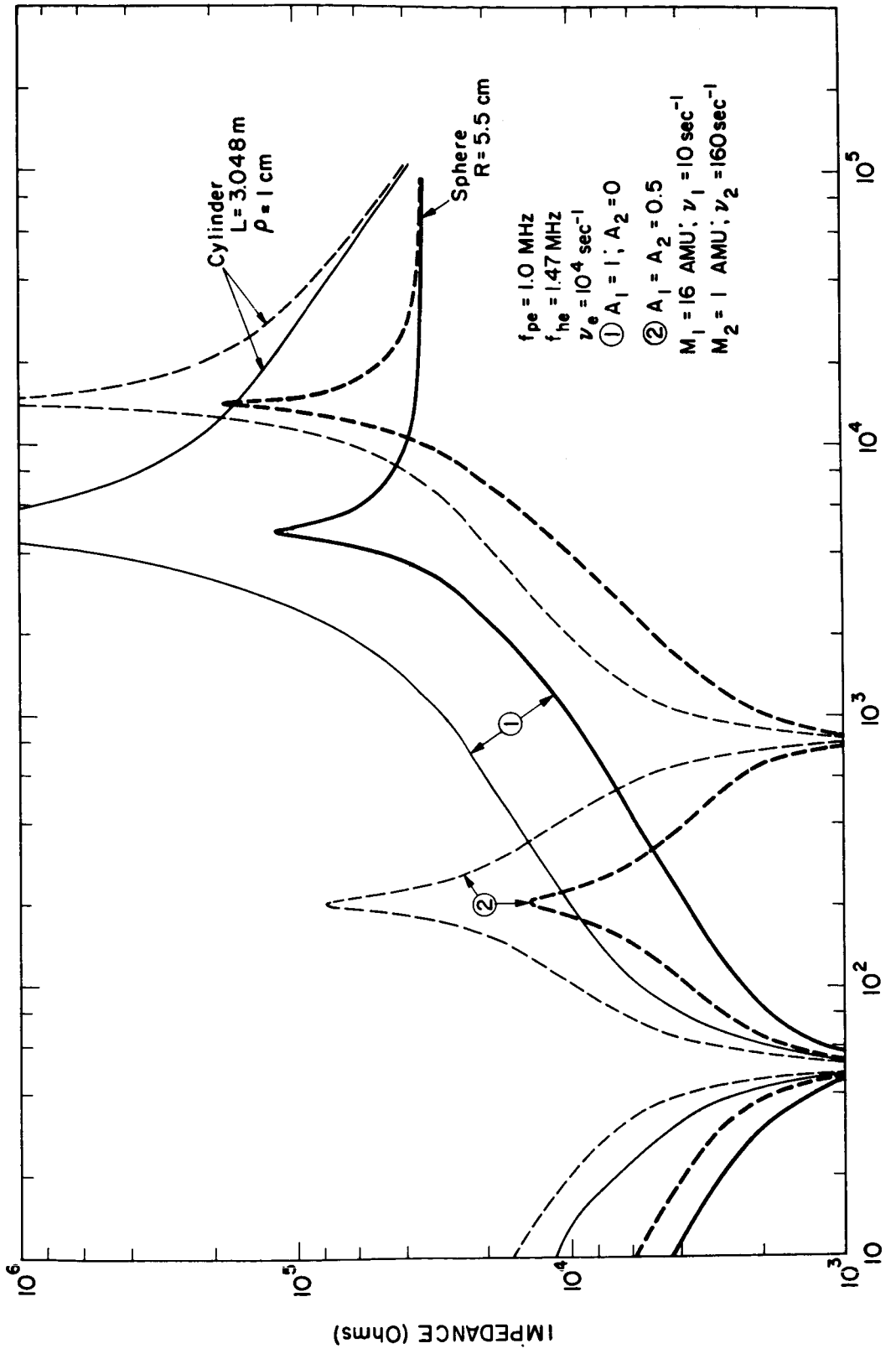

Fig. 1. Impedance of both the cylindrical and spherical antennas as a function of frequency for the sheathless case and for the one and two-ion magnetoplasmas.

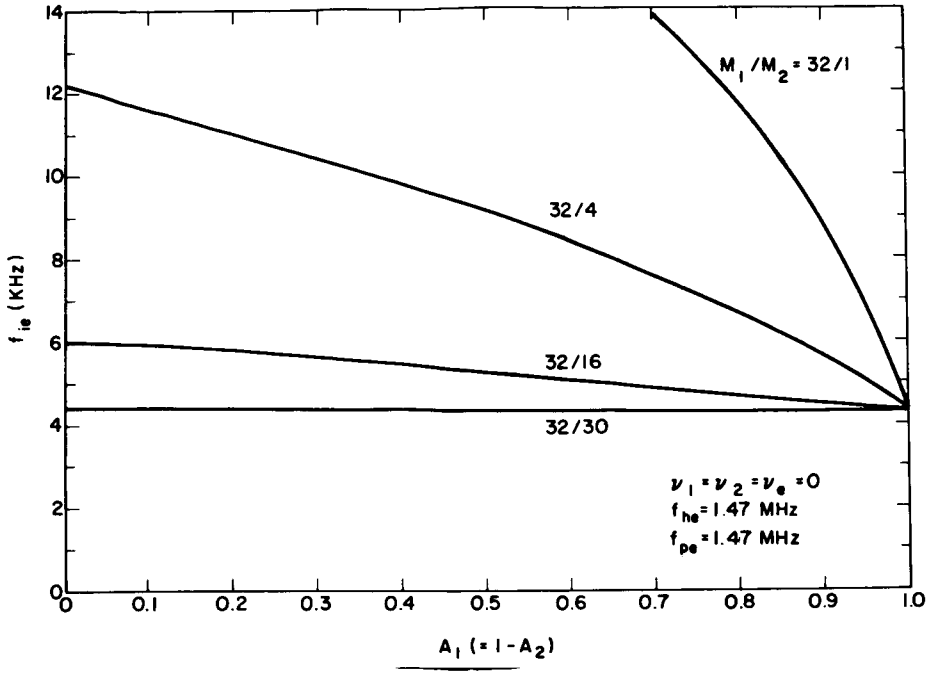

Fig. 2. The two-ion plasma ion-electron hybrid resonance frequency as a function of relative ion abundance with the ion mass ratio a parameter.

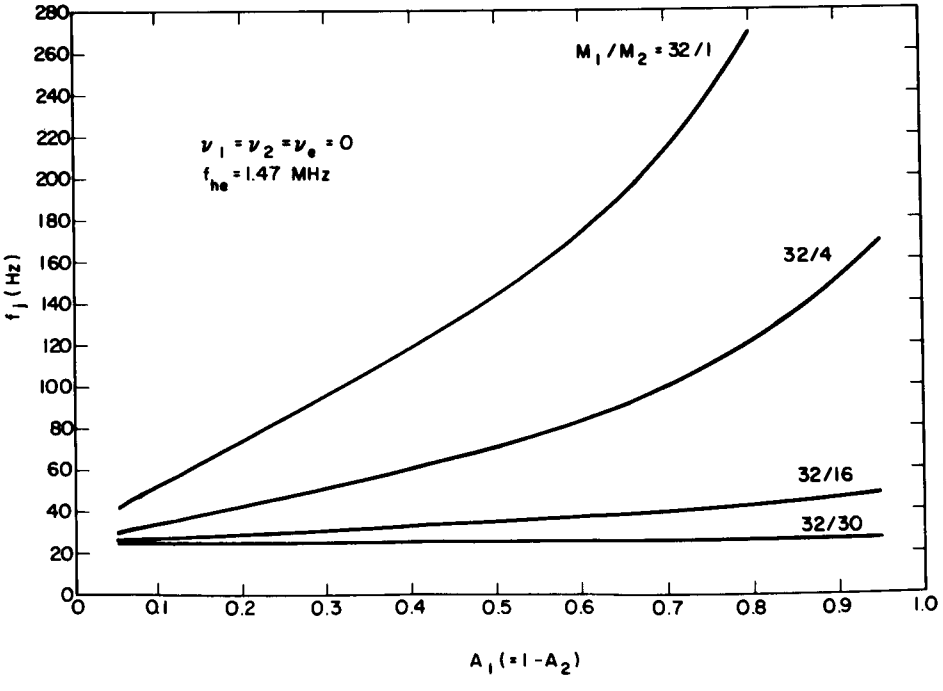

Fig. 3. The two-ion plasma ion-ion hybrid resonance frequency as a function of relative ion abundance with the ion mass ratio a parameter.

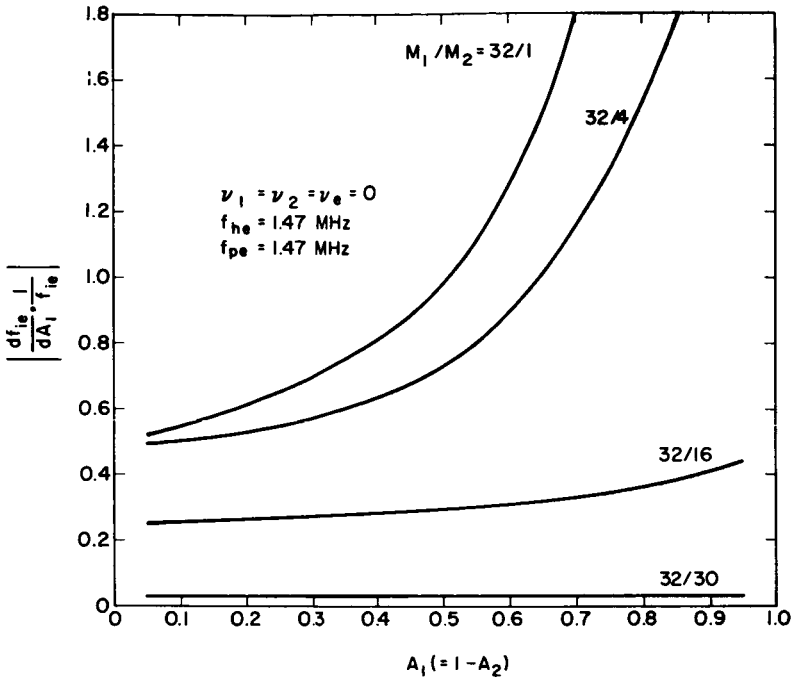

Fig. 4. The two-ion plasma normalized ion-electron hybrid resonance frequency derivative with respect to relative ion abundance with the ion mass ratio a parameter.

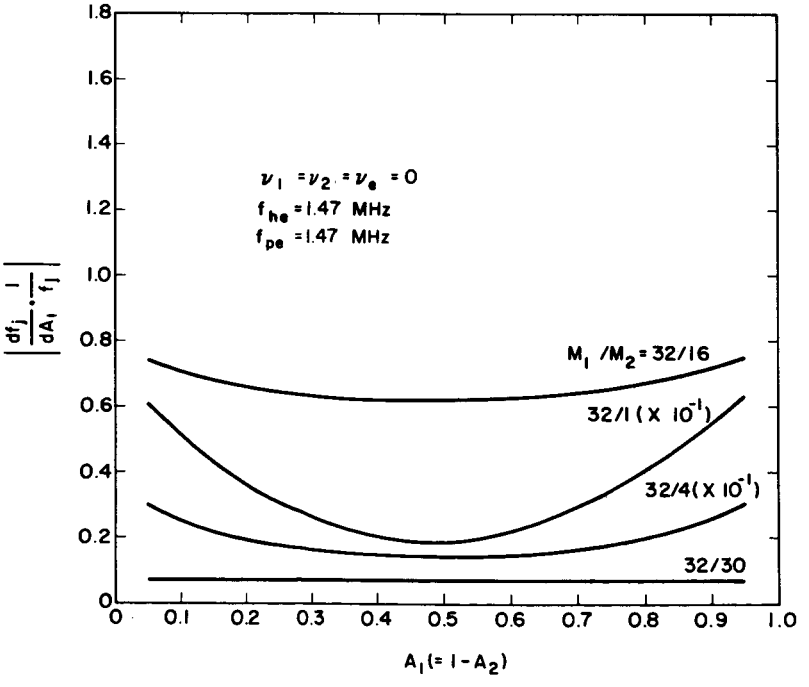

Fig. 5. The two ion plasma normalized ion-ion hybrid resonance frequency derivative with respect to relative ion abundance with the ion mass ratio a parameter.

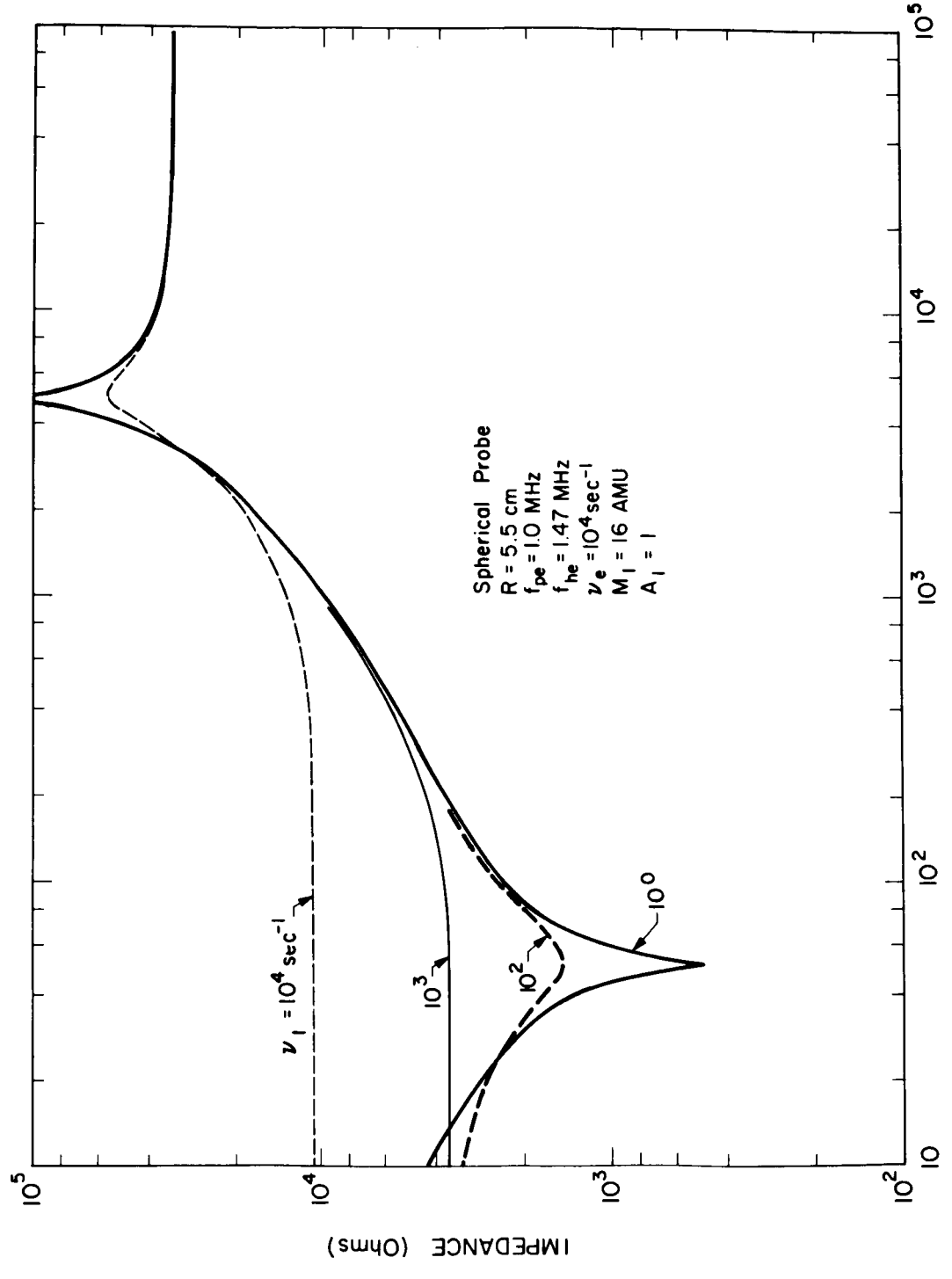

Fig. 6. Spherical probe impedance for the sheathless case in the single ion plasma as a function of frequency with the ion collision frequency a parameter.

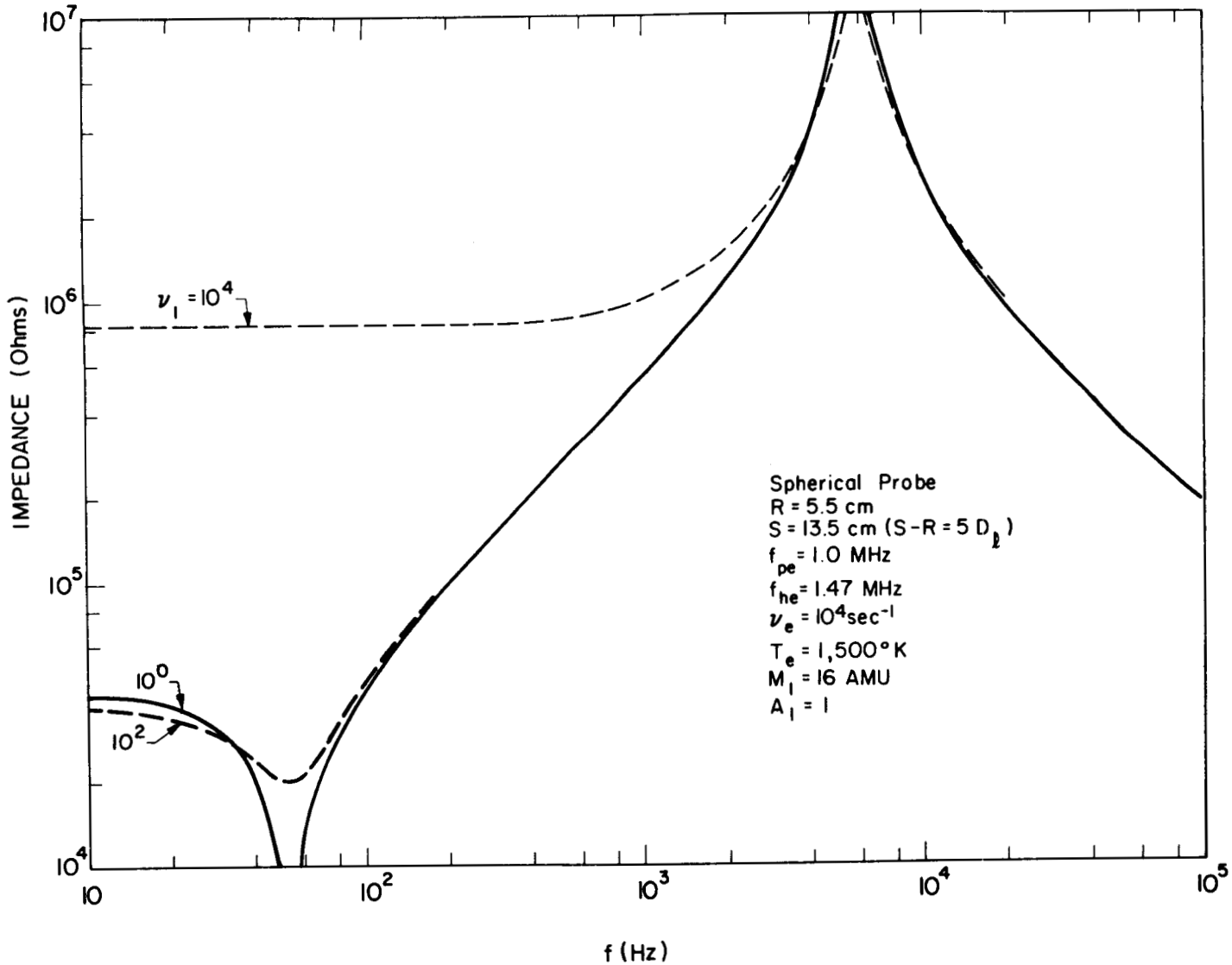

Fig. 7. Spherical probe impedance for the 5 D_ℓ ion sheath and electron temperature of 1, 500°K in the single ion plasma as a function of frequency with the ion collision frequency a parameter.

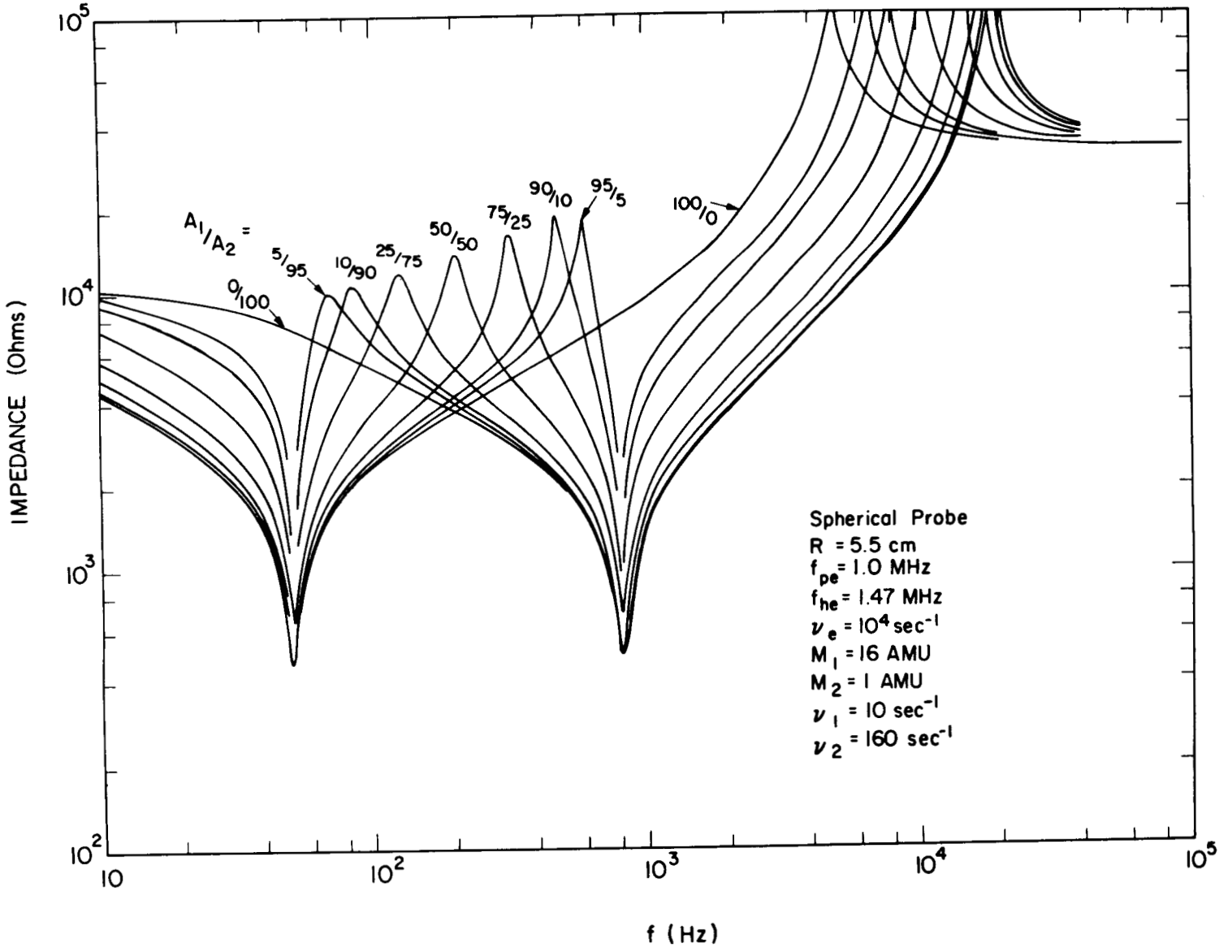

Fig. 8. Impedance of the spherical probe in the two-ion plasma for the sheathless case as a function of frequency with the relative ion abundance ratio a parameter.

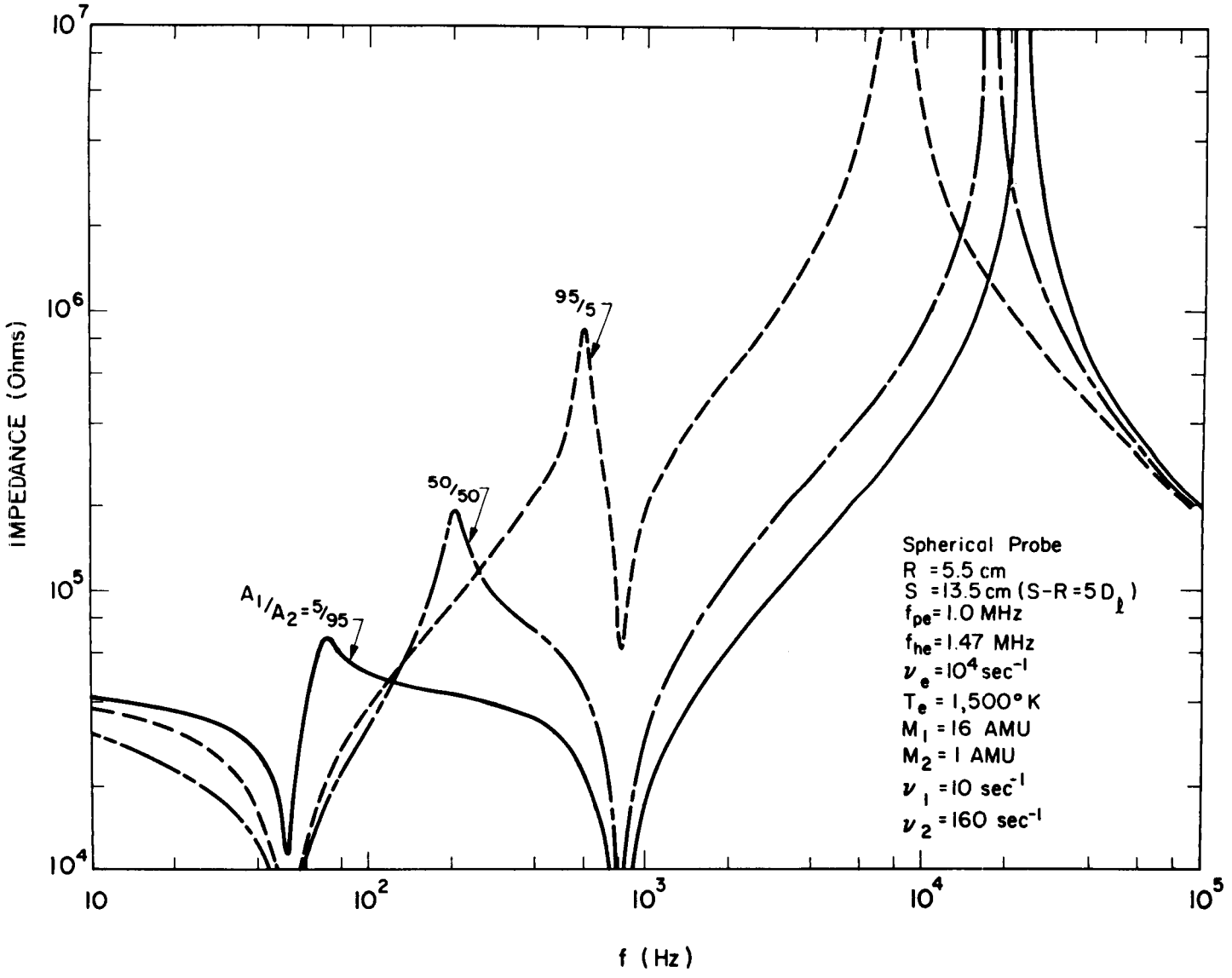

Fig. 9. Impedance of the spherical probe in the two-ion plasma for the 5 D_ℓ ion sheath as a function of frequency, with the relative ion abundance ratio a parameter.

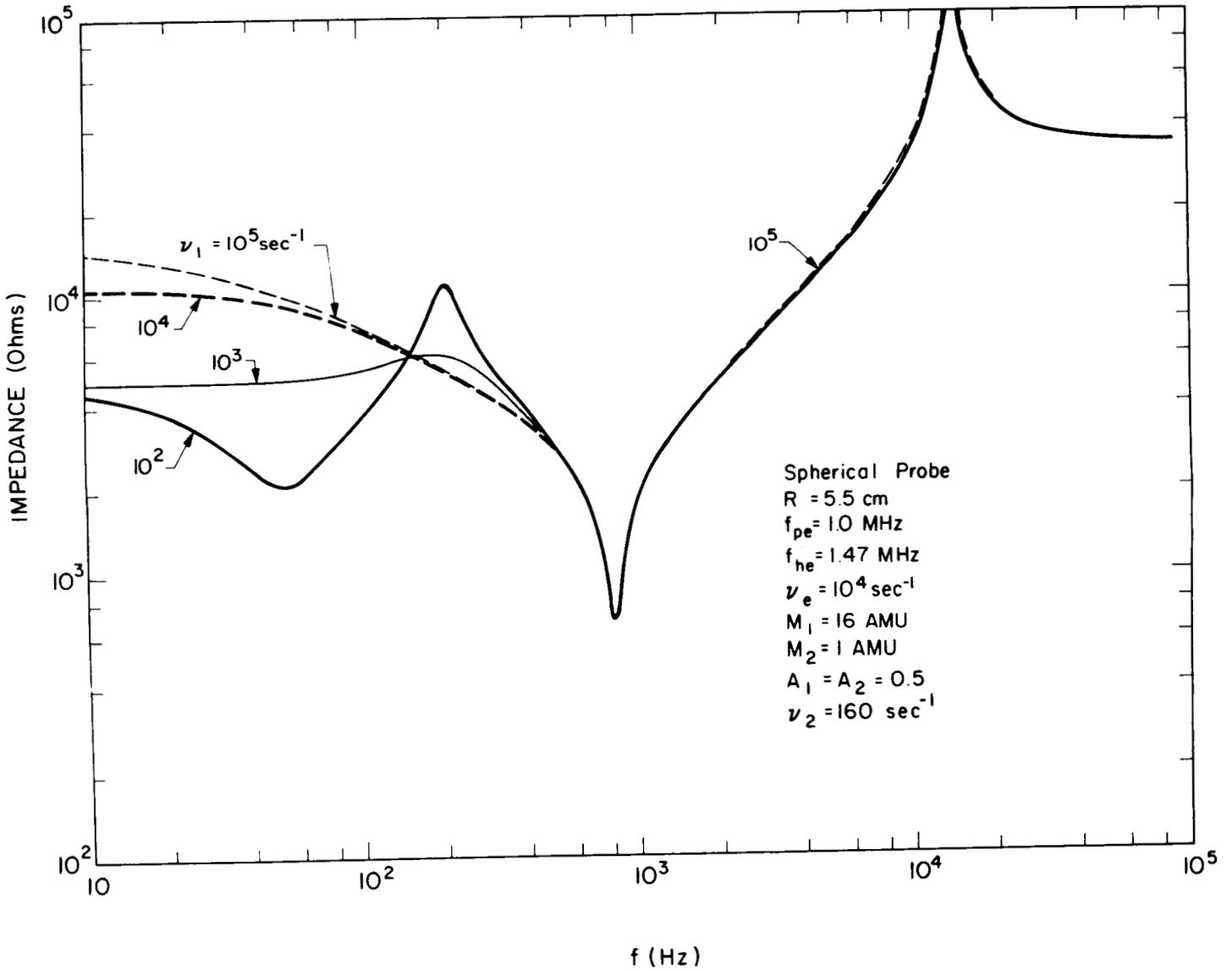

Fig.10. Spherical probe impedance for the two-ion plasma and the sheathless case as a function of frequency with the heavier ion collision fre - quency a parameter.

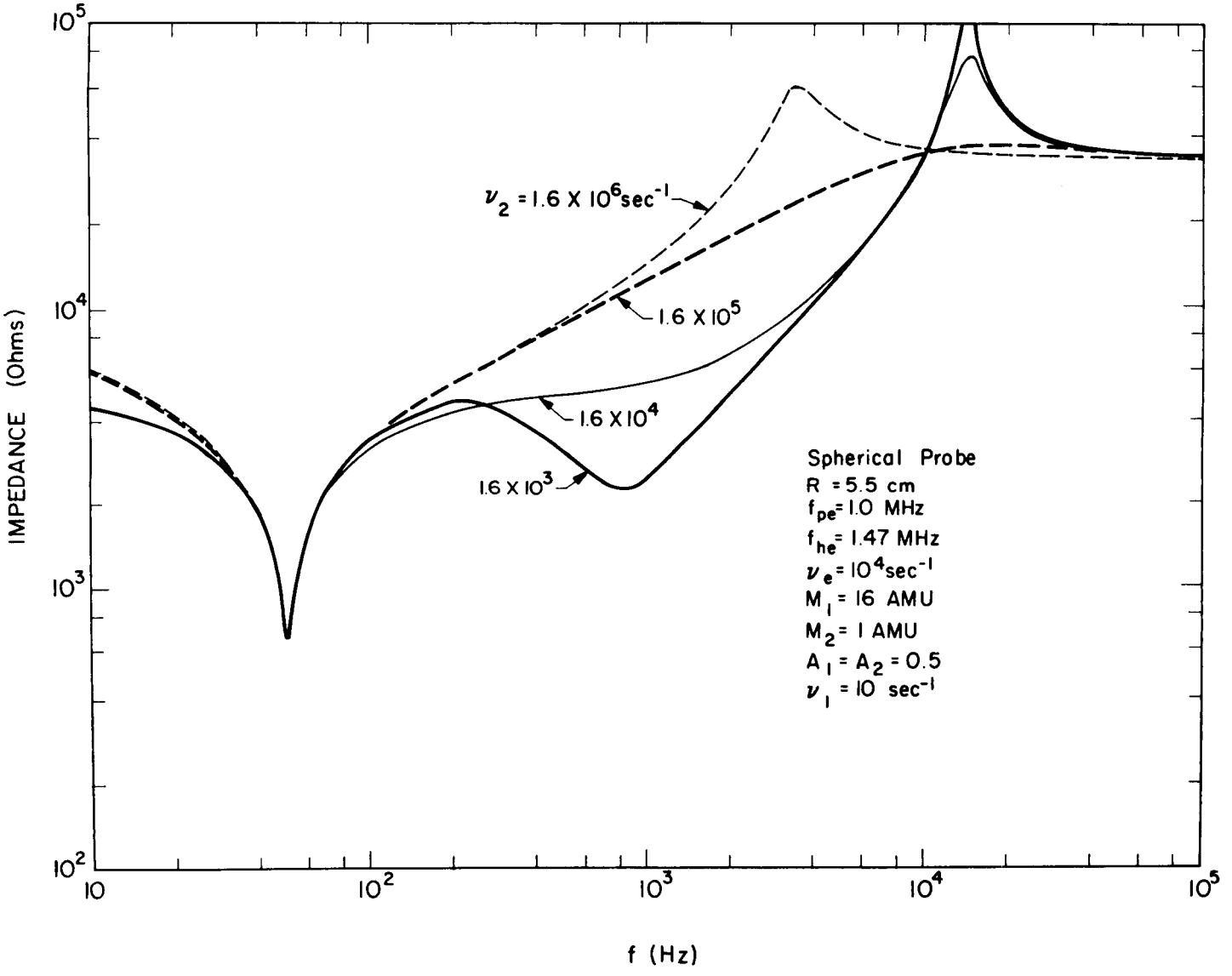

Fig. 11. Spherical probe impedance for the two-ion plasma and the sheathless case as a function of frequency with the lighter ion collision fre - quency a parameter.

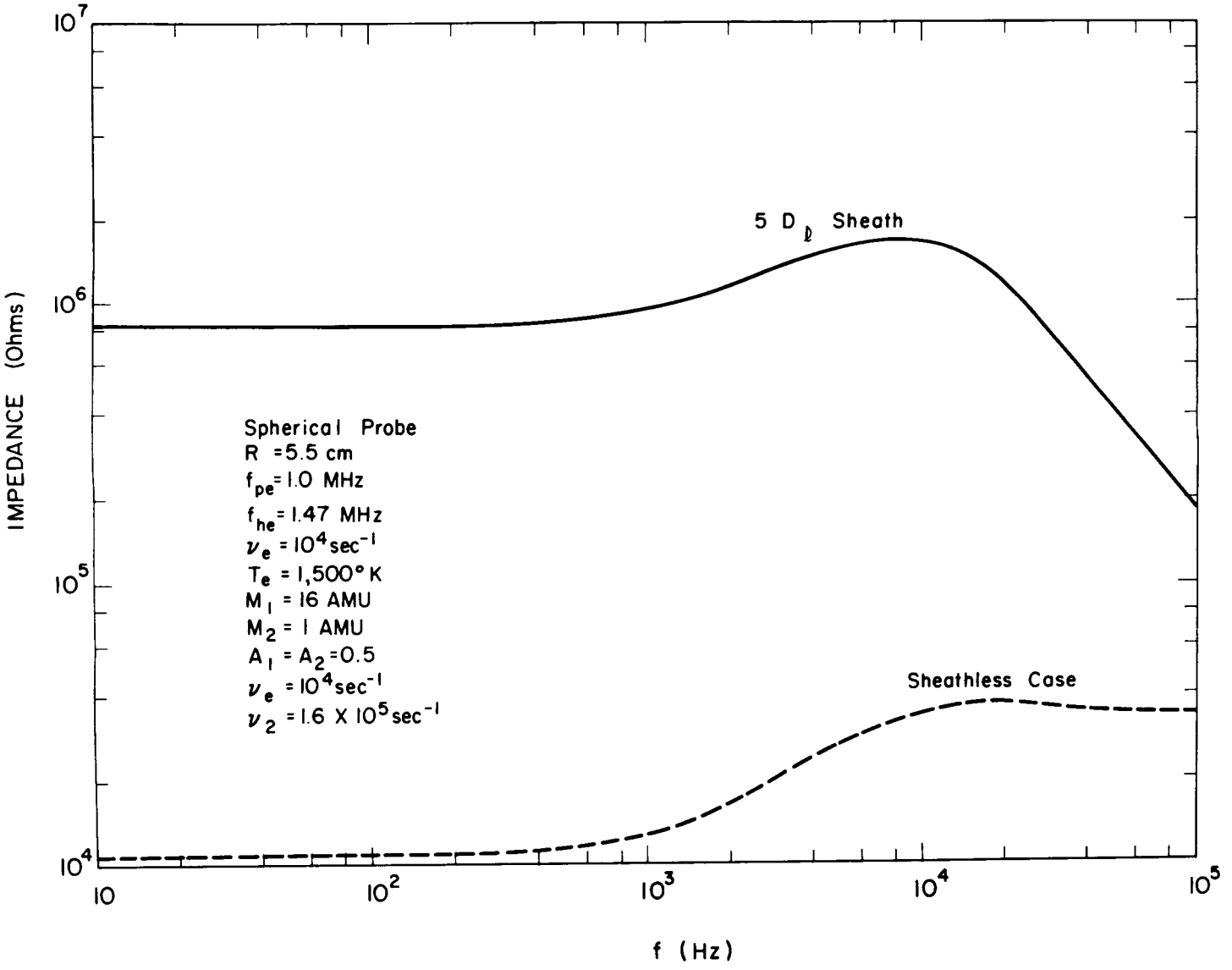

Fig. 12. Spherical probe impedance for the two-ion plasma and both the sheathless case and 5 $D\ell$ ion sheath as a function of frequency.

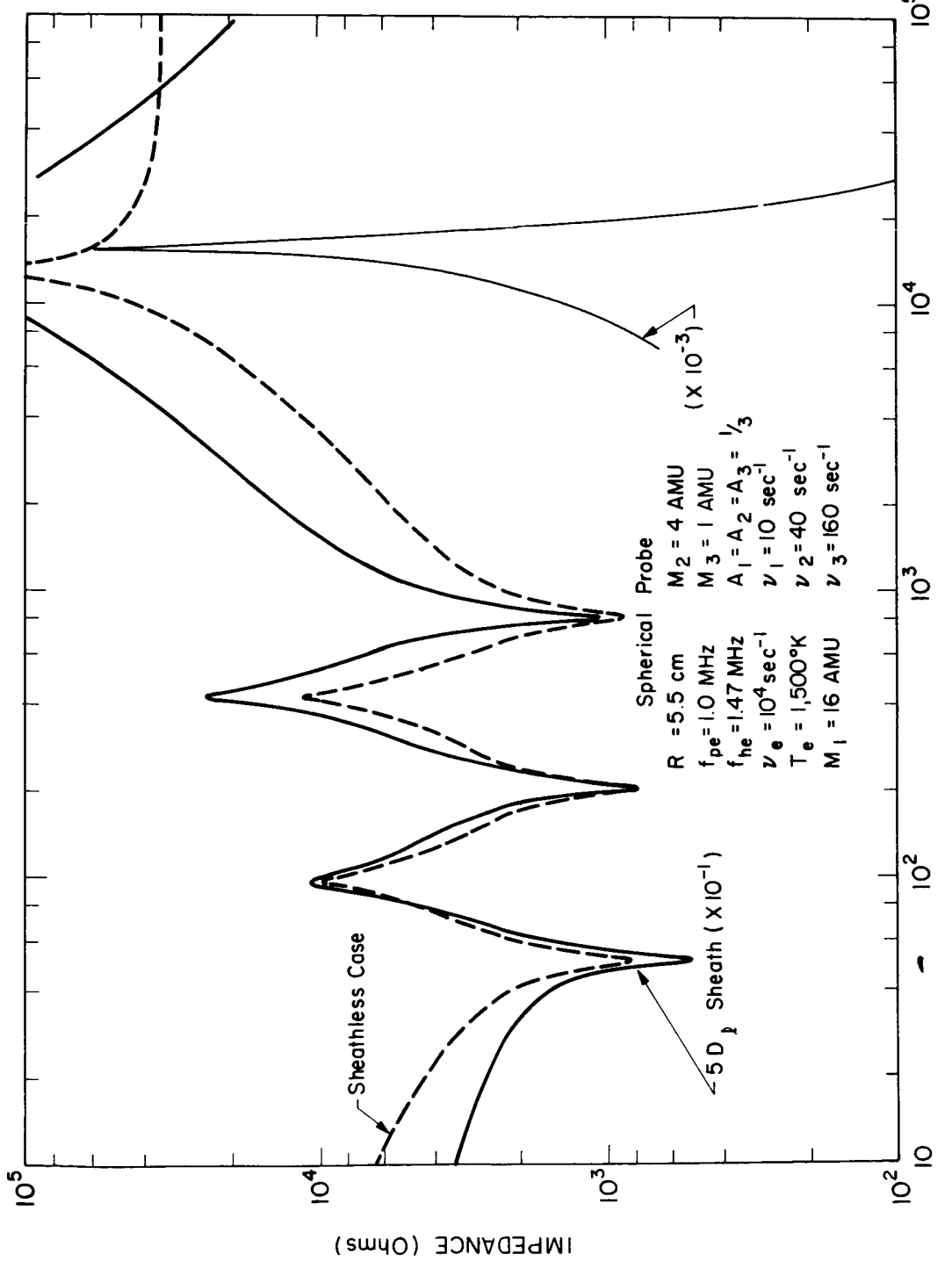

Fig. 13. Impedance of the spherical probe for the three-ion plasma and both the sheathless case and 5 D_ℓ ion sheath as a function of frequency.

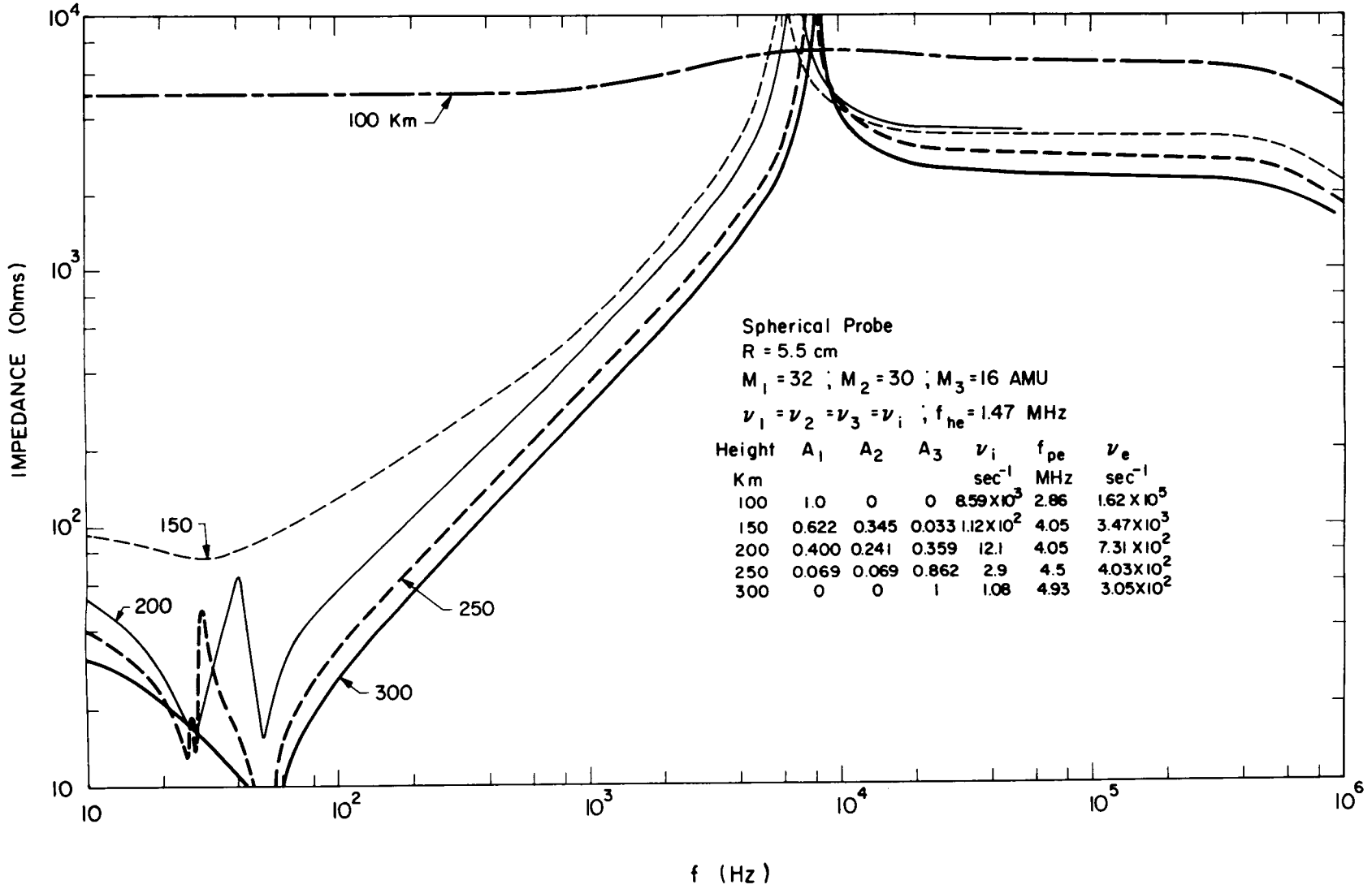

Fig. 14. Impedance of the spherical probe for the sheathless case as a function of frequency for a typical ionosphere containing O_2^+, NO^+ and O^+ ions over the altitude range 100 to 300 km.

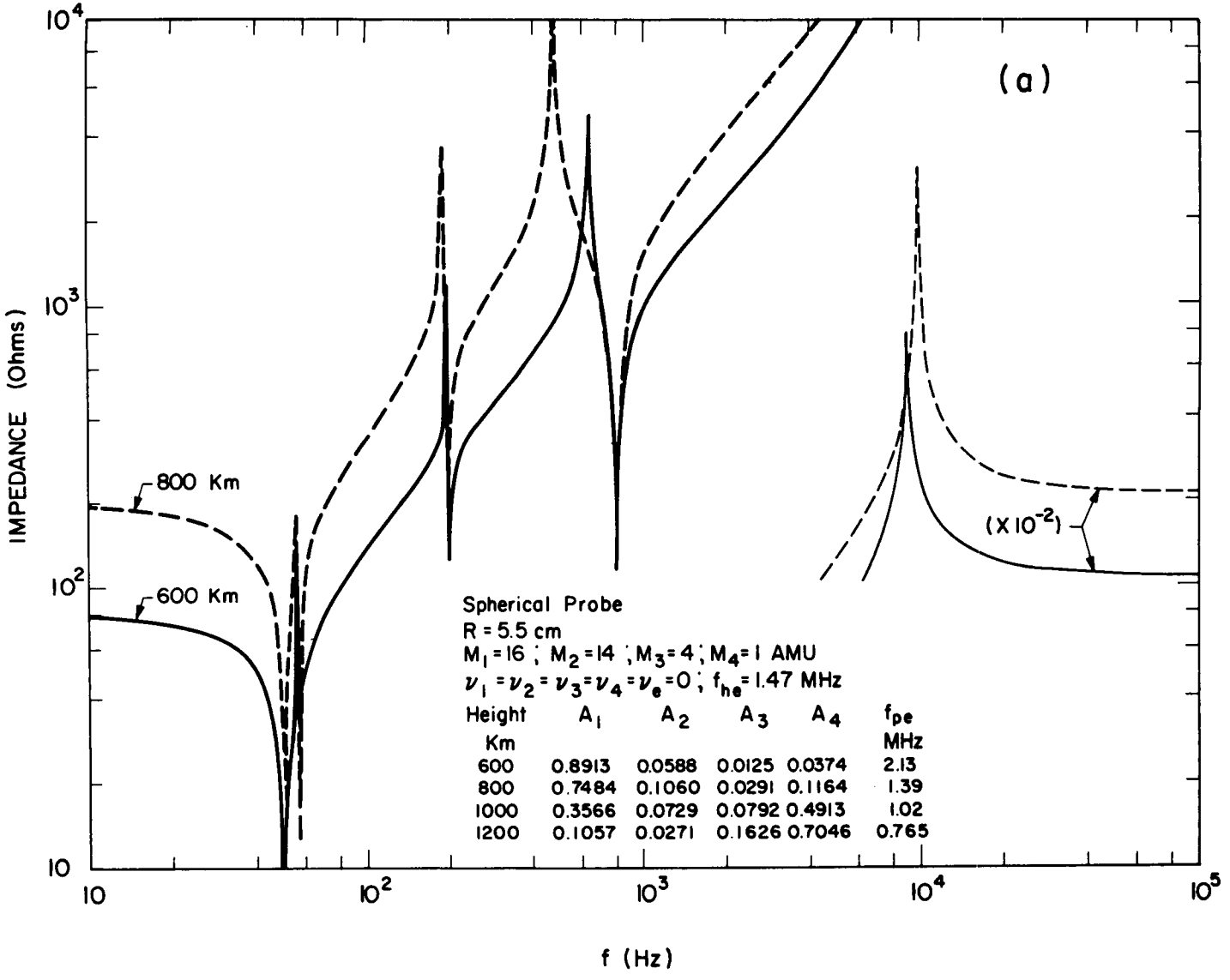

Fig. 15. Impedance of the spherical probe for the sheathless case as a function of frequency for a typical ionosphere containing O^+, N^+, He_2^+ and H^+ ions for the altitudes: (a) 600 and 800 km; and (b) 1, 000 and 1, 200 km.

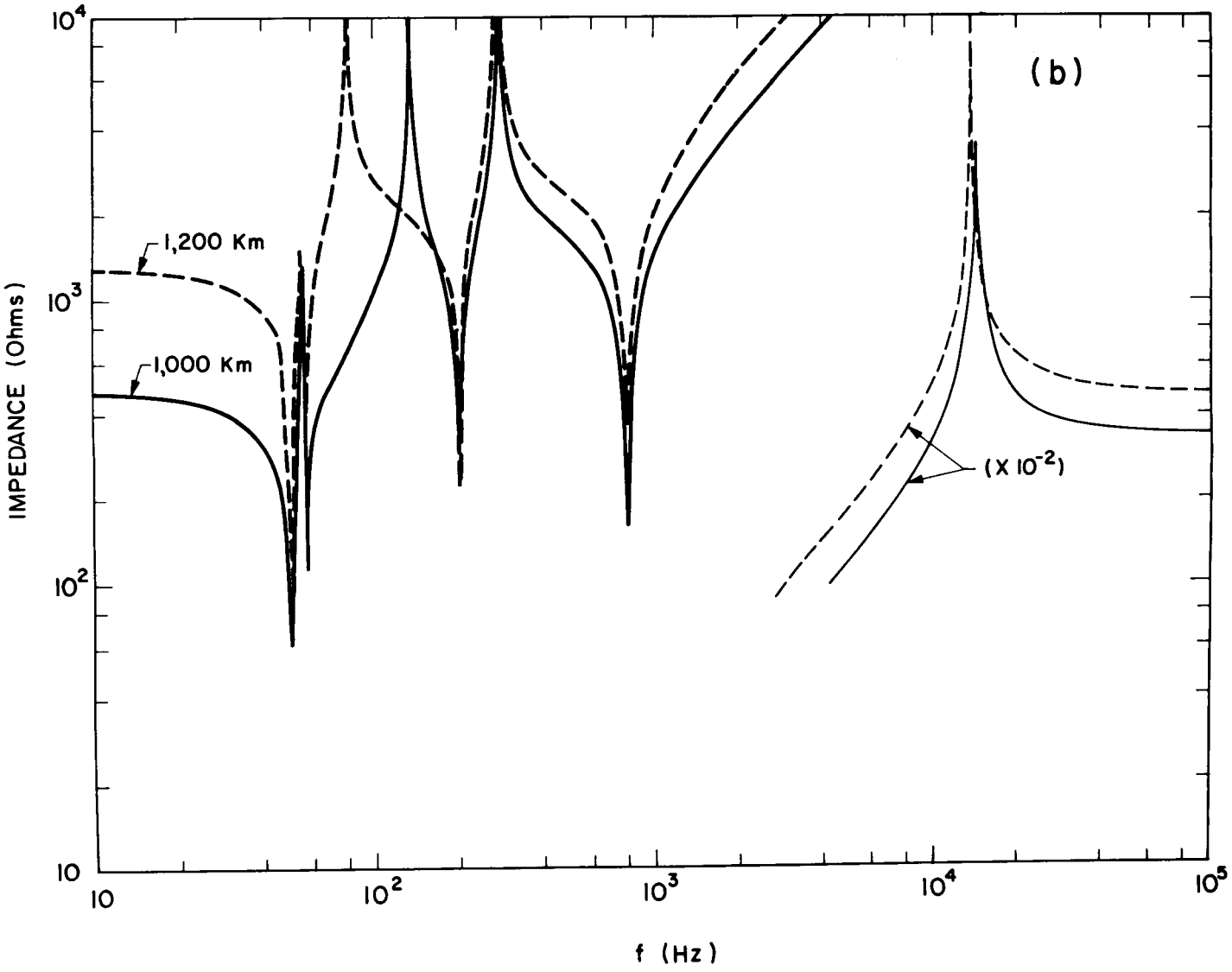

Fig. 15. (Concluded).

References

Aggson, T. L. and C. A. Kapetanko s (1966), "On the Impedance of a Satellite Borne VLF Electric Field Antenna", Report X-612-66-380, Goddard Space Flight Center, Greenbelt, Maryland.

Allis, W. P., S. J. Buchsbaum and A. Bers (1963), "Waves in Anisotropic Plasmas", M. I. T. Press, Cambridge, Mass.

Ament, W. S., J. C. Katzin, M. Katzin and B. Y. -C Koo (1964), "Impedance of a Cylindrical Dipole Having a Sinusoidal Current Distribution in a Homogeneous Anisotropic Ionosphere", Rad. Sci. J. of Res., NBS/USNC-URSI 68D, No. 4, 379-405.

Bachynski, M. P. (1966), "Sources in Unbounded Plasmas", Invited Review Paper, XVth General Assembly of URSI, Munich, Germany; RCA Victor Res. Report No. 7-801-50.

Baldeschwieler, J. D. (1968), "Ion Cyclotron Resonance Spectroscopy", Science, Vol. 159, No. 3812, 263-273.

Balmain, K. G., (1946a, 1964b), "The Impedance of a Short Dipole Antenna in a Magnetoplasma", U. of Illinois, Urbana, Ill., Aeronomy Report No. 2, IEEE Trans. on Ant. and Prop., AP-12, No. 5, 605-617.

Balmain, K. G. (1966), "Impedance of a Spherical Probe in a Magnetoplasma", IEEE Trans. on Ant. and Prop., AP-14, No. 3, 402-403.

Balmain, K. G., G. Oksiutik and J. Fejer (1967), "RF Probe Admittance in the Ionosphere: Comparison of Theory and Experiment", Spring URSI Meeting, Ottawa, Ontario, Canada.

Blair, W. E., (1968), "Ionospheric Diagnostics Using Resonances of an Electric Dipole Impedance", Radio Science, Vol. 3, No. 2, 155-161.

Brice, N. M. (1965), "Ion Effects Observed in Radio Wave Propagation in the Ionosphere", URSI Symposium on Electromagnetic Wave Theory, Delft, Netherlands.

Chapman, S. (1956), "The Electrical Conductivity of the Ionosphere: a Review", Suppl. to Vol. IV, Series X, Nuovo Cimento, No. 4, 1385-1412.

Chu, C. M., J. LaRue and D. B. van Hulsteyn (1966), "Investigations on Excitation and Propagation in Ionized Media", Rome Air Development Center, Report No. RADC-TR-65-484.

Dougherty, J. P. and J. J. Monaghan (1966), "Theory of Resonances Observed in Ionograms Taken by Sounders Above the Ionosphere", Proc. Royal Soc. Series A, 289, 214-234.

Fejer, J. A. and W. Calvert (1964), "Resonance Effects of Electrostatic Oscillations in the Ionosphere", J. Geophy. Res., 69, No. 23, 5049-5062.

Galejs, J. (1966a), "Impedance of a Finite Insulated Cylindrical Antenna in a Cold Plasma with a Lonitudinal Magnetic Field", IEEE Trans. on Ant. and Prop., AP-14, No. 6, 727-736.

Galejs, J. (1966b), "Impedance of a Finite, Insulated Antenna in a Cold Plasma with a Perpendicular Magnetic Field", IEEE Trans. on Ant. and Prop., AP-14, No. 6, 737-748.

Ghosh, S.N. (1967), "Ionospheric Characteristics from Altitude Variations of Positive Ion Densities ", U. of Mich. Scientific Report 05627-9-S.

Herman, J.R. (1964), "A Method for Determining D Region Electron-Density Profiles Utilizing a Capacitive Impedance Rocket Probe", J. of Geophys. Res., 69, No. 11, 2329-2336.

Johnson, C.Y., E.B. Meadows and J.C. Holmes (1958), "Ion Composition of the Arctic Ionosphere", J. Geophys. Res., 63, 443-444.

Meyer, P. (1967), "Impedance of a Sphere in a Magnetoplasma", IEEE Trans. on Ant. and Prop., AP-15, No. 2, 331-332.

Miller, E.K. (1967a), "Admittance of the Infinite Cylindrical Antenna in a Lossy Plasma II. The Incompressible Magnetoplasma", U. of Mich. Scientific Report 05627-11-S.

Miller, E.K. and H.F. Schulte, Jr. (1968), "Antenna Admittance in an Ionospheric-Type Plasma", Plasma Waves in Space and the Laboratory, Proceedings of the NATO Advanced Study Institute, Roros, Norway, April, 1968, and U. of Mich. Scientific Report 05627-18-S.

Pyati, V.P. (1966), "Determination of Capacitance in Anisotropic Media", IEEE Trans. on Ant. and Prop., AP-14, No. 6, 803.

Schultz, F.V. and R.W. Groff (1966), "The Radiation Produced by an Arbitrarily Oriented Dipole in an Infinite, Homogeneous, Warm, Anisotropic Plasma", Purdue Univ., TR-EE66-22.

Seshadri, S.R. (1965a), "Radiation Resistance of a Linear Current Filament in a Simple Anisotropic Medium", IEEE Trans. AP-13, No. 5, 819-820.

Seshadri, S.R. (1965b), "Radiation Resistance of Elementary Electric Current Sources in a Magnetoionic Medium", Proc. IEE 112, No. 10, 1856-1868.

Seshadri, S.R. (1966a), "Radiation from a Current Strip in a Uniaxially Anisotropic Plasma Medium", Can. J. Phys. 44, 207-217.

Seshadri, S.R. (1966b), "Effect of Insulation on the Radiation Resistance of an Electric Dipole in a Simple Anisotropic Medium", Proc. IEE 113, No. 4, 593-600.

Shawhan, S.D. and D.A. Gurnett (1967), "Preliminary Results from the Javelin 8.45 VLF Rocket Experiment", U. of Iowa 67-60 Preliminary Report.

Smith, R.L. and N. Brice (1964), "Propagation in Multicomponent Plasmas", J. of Geophys. Res., 69, No. 23, 5029-5040.

Toepfer, A.J. and G.G. Comisar (1966), "Observations of a Resonance Probe Effect Near the Ion Plasma Frequency", Presented at the Fall Meeting of the Division of Plasma Physics, American Physical Society, Boston, Mass.